JOURNAL OF GEOPHYSICAL RESEARCH, VOL. 112, C06014, doi:10.1029/2006JC003947, 2007

Click Here for Full Article

Sea surface temperature signatures of oceanic internal waves in low winds

J. Thomas Farrar,[1,2] Christopher J. Zappa,[3] Robert A. Weller,[4] and Andrew T. Jessup[5]

Received 28 September 2006; revised 17 January 2007; accepted 26 February 2007; published 20 June 2007.

[1] In aerial surveys conducted during the Tropical Ocean–Global Atmosphere Coupled Ocean-Atmosphere Response Experiment and the low-wind component of the Coupled Boundary Layer Air-Sea Transfer (CBLAST-Low) oceanographic field programs, sea surface temperature (SST) variability at relatively short spatial scales (O(50 m) to O(1 km)) was observed to increase with decreasing wind speed. A unique set of coincident surface and subsurface oceanic temperature measurements from CBLAST-Low is used to investigate the subsurface expression of this spatially organized SST variability, and the SST variability is linked to internal waves. The data are used to test two previously hypothesized mechanisms for SST signatures of oceanic internal waves: a modulation of the cool-skin effect and a modulation of vertical mixing within the diurnal warm layer. Under conditions of weak winds and strong insolation (which favor formation of a diurnal warm layer), the data reveal a link between the spatially periodic SST fluctuations and subsurface temperature and velocity fluctuations associated with oceanic internal waves, suggesting that some mechanism involving the diurnal warm layer is responsible for the observed signal. Internal-wave signals in skin temperature very closely resemble temperature signals measured at a depth of about 20 cm, indicating that the observed internal-wave SST signal is not a result of modulation of the cool-skin effect. Numerical experiments using a one-dimensional upper ocean model support the notion that internal-wave heaving of the warm-layer base can produce alternating bands of relatively warm and cool SST through the combined effects of surface heating and modulation of wind-driven vertical shear.

Citation: Farrar, J. T., C. J. Zappa, R. A. Weller, and A. T. Jessup (2007), Sea surface temperature signatures of oceanic internal waves in low winds, *J. Geophys. Res.*, *112*, C06014, doi:10.1029/2006JC003947.

1. Introduction

[2] Infrared (IR) imagery of the sea surface reveals a rich variety of patterns and coherent features at scales ranging from the centimeter scales of "microbreaking" waves to basin scales. While many investigations have focused on either the smaller scales associated with surface wave processes [e.g., *Simpson and Paulson*, 1980; *Jessup and Hesany*, 1996; *Jessup et al.*, 1997a, 1997b; *Zappa et al.*, 2001, 2004; *Marmorino and Smith*, 2005] or larger scales associated with meso- and basin-scale dynamics [e.g., *Stumpf and Legeckis*, 1977; *Apel*, 1980; *Hill et al.*, 2000; *Farrar and Weller*, 2006], a handful of recent papers have reported internal-wave signals in infrared observations [*Walsh et al.*, 1998; *Marmorino et al.*, 2004; *Zappa and Jessup*, 2005]. Yet, adiabatic internal wave theory suggests that there should be no internal-wave signal in sea surface temperature (SST), since a fluid element initially at the surface remains there for all time. More than one mechanism has been put forward to explain the existence of propagating SST signals associated with internal waves. Aside from the potentially important effects of this SST modulation on air-sea exchange and the atmospheric boundary layer, it is of interest to better understand these effects for remote sensing applications, both for remote measurement of internal waves and for understanding potential contamination of large-scale satellite estimates of SST by the smaller-scale internal wave signals.

[3] This paper uses data collected during the low-wind component of the Coupled Boundary Layer Air-Sea Transfer experiment (CBLAST-Low) [*Edson et al.*, 2007] to examine the surface infrared signatures of oceanic internal waves and the mechanisms for these signatures. In addition to measurements of air-sea fluxes of heat, momentum, and moisture, this paper makes use of a unique data set consisting of collocated high-resolution airborne infrared imagery,

[1]Massachusetts Institute of Technology/Woods Hole Oceanographic Institution Joint Program in Oceanography, Woods Hole, Massachusetts, USA.
[2]Now at Department of Physical Oceanography, Woods Hole Oceanographic Institution, Woods Hole, Massachusetts, USA.
[3]Lamont-Doherty Earth Observatory, Columbia University, Palisades, New York, USA.
[4]Department of Physical Oceanography, Woods Hole Oceanographic Institution, Woods Hole, Massachusetts, USA.
[5]Applied Physics Laboratory, University of Washington, Seattle, Washington, USA.

Copyright 2007 by the American Geophysical Union.
0148-0227/07/2006JC003947$09.00

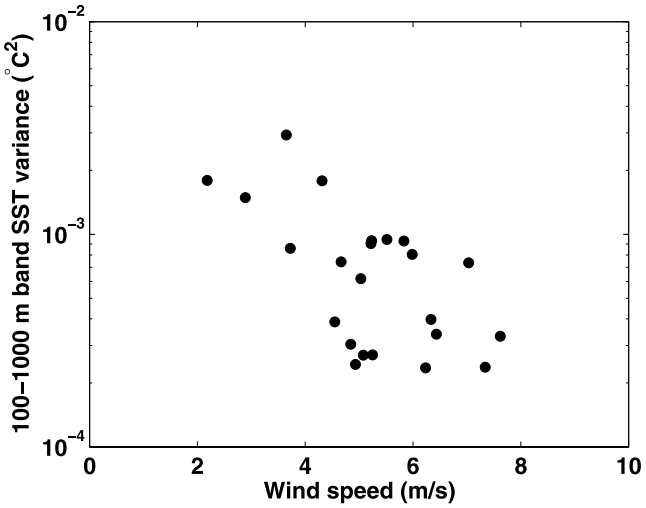

Figure 1. Surface temperature variance at 100- to 1000-m along-track scales from airborne infrared observations collected during the CBLAST-Low experiment (section 3) versus mean wind speed during each flight.

shipboard infrared measurements, towed thermistor-chain measurements, and moored measurements of temperature and velocity.

[4] *Osborne* [1965] predicted that internal waves (as well as surface waves) should have a signal in SST, because vertical straining of the sea surface is expected to modify the magnitude of the cool-skin effect. (The cool skin is an O(1 mm)-thick conductive boundary layer that is cooler than the bulk fluid below because of latent, sensible, and long-wave heat loss from the sea surface [*Katsaros*, 1980]. *Osborne*'s [1965] theoretical work is remarkable in part because the theory preceded, but is consistent with, the canonical model of the cool skin later offered by *Saunders* [1967].

[5] *Walsh et al.* [1998] observed quasiperiodic, propagating variations in IR SST measurements and argued that the variations were associated with oceanic internal waves. They proposed that the internal waves modulate vertical mixing within the strongly stratified layer that forms in the upper few meters during conditions of strong insolation and low winds. This interpretation was supported by the fact that nearby mooring data showed that internal waves caused temperature fluctuations as shallow as 0.5 m depth, but there were no coincident surface and subsurface measurements to unambiguously confirm the proposed mechanism.

[6] *Marmorino et al.* [2004] observed quasiperiodic, propagating variations in IR imagery and interpreted these as being associated with internal waves. *Marmorino et al.* [2004] invoked a variation of *Osborne*'s [1965] theory to account for the signal, but there were no subsurface data to corroborate this interpretation. *Zappa and Jessup* [2005] also observed spatially periodic structure in IR imagery and used nearby mooring data to argue that the signal was due to (nonlinear) internal waves; *Zappa and Jessup* [2005] appealed to the cool-skin straining mechanism [*Osborne*, 1965; *Marmorino et al.*, 2004] as a likely explanation of the signal.

[7] The data of *Walsh et al.* [1998] and *Marmorino et al.* [2004] were collected in similar weather conditions. Both aerial surveys were carried out during the afternoon (13:00–18:00 local time) with wind speeds below 3 m/s. *Zappa and Jessup* [2005] also presented data collected in low winds, but their survey was conducted in the morning, around 07:00 (local time). The observations examined in this study were also collected in low winds.

[8] It remains an open question whether internal-wave signals in SST occur only under low winds, but *Hagan et al.* [1997] and *Walsh et al.* [1998] noted that internal-wave-scale patterns were observed in SST under low-wind conditions during the Tropical Ocean–Global Atmosphere (TOGA) Coupled Ocean-Atmosphere Response Experiment (COARE). In the CBLAST-Low experiment, we have qualitatively observed an increase of SST variability at internal-wave scales as wind speed decreases. For example, Figure 1 shows SST variance in the 100- to 1000-m wavelength band versus mean wind speed for 23 aerial SST surveys carried out during CBLAST-Low. A tendency for increased SST variance at internal-wave scales during low winds is apparent, but we note that the relationship between wind speed and SST variance depicted in Figure 1 may be affected by the fact that different missions were carried out by the aircraft during the course of the experiment. In particular, sampling patterns were designed for each mission based in part on wind speed and SST variability.

[9] An example of the small-scale SST variability seen in low winds during the CBLAST-Low experiment is shown in Figure 2. These data were collected on August 15, 2003, the day corresponding to the point of largest 100- to 1000-m-scale SST variance in Figure 1. The particular image shown in Figure 2 was selected because one of the surface moorings used in this study is visible in the image, but the SST signal is typical of what is observed and is similar to the signals seen in data presented by *Marmorino et al.* [2004].

[10] This paper is organized as follows. Section 2 gives some details of the previously hypothesized mechanisms for the existence of internal-wave signals in SST and discusses our approach to testing these hypotheses using field data. Section 3 describes the data set and experimental design. In section 4, the data are analyzed to examine the subsurface expression of the SST signal. Section 5 discusses the implications of the observations for the hypothesized mechanisms. Section 6 presents conclusions.

2. Theory

[11] The conditions considered by *Walsh et al.* [1998] and *Marmorino et al.* [2004] were similar to those during the afternoon survey described here (section 3). All three sets of infrared skin-temperature measurements were collected during the afternoon (13:00–18:00 local time) under conditions of light winds ($<\sim$3 m/s), and all three data sets suggest the presence of spatially organized SST fluctuations associated with internal waves. Although these similarities suggest that the same mechanism may be responsible for the internal-wave signal observed in SST, *Walsh et al.* [1998] and *Marmorino et al.* [2004] proposed different hypotheses for the existence of the signal. *Marmorino et al.* [2004] suggested that the internal-wave signal resulted

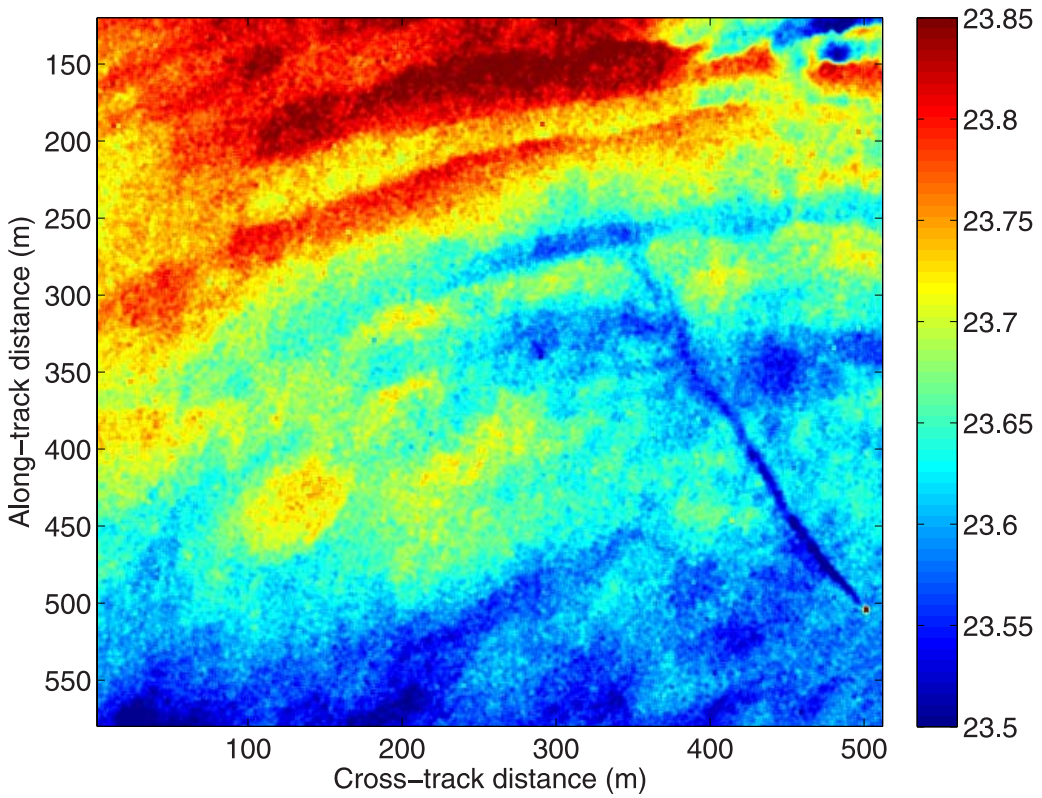

Figure 2. SST (°C). This is an example of quasiperiodic SST variability that is likely associated with internal waves. The data come from the airborne infrared measurements described in section 3. The plane's heading was nearly due north. One of the IMET buoys is visible in the lower right corner as a warm circle with a long, cool wake trailing to the northwest. The buoy is warmer than the surrounding water because of radiant heating in the afternoon sun and low winds, and the wake is cool because the O(1 m)-thick stratified warm layer has been disrupted by the flow past the buoy.

from modulation of the O(1 mm)-thick cool skin on the ocean surface, while *Walsh et al.* [1998] hypothesized that the SST signal resulted from modulation of the entrainment rate at the base of the diurnal warm layer (of O(1 m) thickness). An illuminating discussion of both the cool-skin and warm-layer effects is given by *Fairall et al.* [1996b]. The goal of this study is to evaluate these two hypotheses using the coincident observations of skin temperature and subsurface temperature collected during the CBLAST-Low field campaign. Here we give more detail about the type of surface signal expected under these two hypotheses.

2.1. Cool-Skin Straining

[12] *Marmorino et al.* [2004] hypothesized that the internal-wave signal observed in IR SST measurements was due to cool-skin straining, based in part on the theoretical work of *Osborne* [1965], who offered a comprehensive study of the SST signal expected in a wide range of strain conditions, covering order-of-magnitude variations in amplitude and frequency of strain-rate fluctuations. We will first summarize the effect of internal-wave straining on the cool skin predicted by *Marmorino et al.* [2004] before reviewing the more general theory of *Osborne* [1965].

[13] To estimate the effect of a fluctuating surface strain rate on the ocean skin temperature, *Marmorino et al.* [2004] employed a linearized version of a model equation for the steady-state behavior of the cool skin in the presence of a positive surface strain [*Leighton et al.*, 2003, equation (4.6)], noting that this equation is similar to equation (19) of *Osborne* [1965]. The equation used by *Marmorino et al.* [2004] is

$$\Delta T = \sqrt{\frac{\pi}{2\kappa\alpha}}\left(\frac{Q}{\rho c_p}\right), \tag{1}$$

where α is the horizontal surface divergence (i.e., vertical strain rate; $\alpha \equiv -\partial w/\partial z$), κ is the molecular diffusivity of heat, Q is the surface heat flux applied to the skin layer, ρ is the water density, and c_p is the specific heat. The approach of *Marmorino et al.* [2004] for predicting the skin temperature response to variations in the strain rate from internal waves was to use estimates of ΔT and Q from observations to estimate the ambient strain rate from equation (1), finding $\alpha \approx 0.05\ \mathrm{s}^{-1}$. Then, equation (1) was linearized about this value. Using the linearized equation,

$$T' = \alpha_{IW}\frac{\partial \Delta T}{\partial \alpha}, \tag{2}$$

Marmorino et al. [2004] suggested that an oscillatory strain field of amplitude $\alpha_{IW} = 0.01\ \mathrm{s}^{-1}$ would be sufficient to produce the observed SST variations. *Marmorino et al.*

[2004] asserted that $\alpha_{IW} = 0.01\ s^{-1}$ is a reasonable value for the internal-wave strain amplitude at the surface, but there were no concurrent in situ observations to support this claim. We note here that this strain rate implies a vertical velocity on the order of 1 cm/s at a depth of 1 m.

[14] The hypothesis that internal waves modulate the magnitude of the cool-skin effect is plausible, but use of equation (1) to estimate the magnitude of this effect is potentially problematic. As one might guess from the infinitely cold skin that equation (1) gives for zero strain, this model solution is not appropriate for small strain values. *Osborne* [1965] states this explicitly in his discussion of his equation (19); the solution is appropriate for values of α that satisfy $\alpha \gg \frac{\kappa}{\delta^2} \approx 0.1\ s^{-1}$ (δ is the thickness of the cool skin), where the approximate equality is obtained using $\kappa \approx 10^{-7}\ m^2/s$ and $\delta \approx 1$ mm. Thus the ambient strain rate of $0.05\ s^{-1}$ that *Marmorino et al.* [2004] inferred using equation (1) is potentially outside of the range for which the equation is applicable, so the estimated sensitivity is possibly too large. *Marmorino et al.* [2004] claimed that the extreme sensitivity of equation (1) to strain-rate variations at low strain values, coupled with low ambient strain values, is the reason that an internal-wave signal is detectable in the skin temperature. We find this claim dubious because inspection of equation (1) suggests impossibly large (i.e., infinite) skin temperature signals when there is no background strain field. In order to evaluate the hypothesis that internal waves produce a signal in the skin temperature via straining of the cool skin, we now review the model of *Osborne* [1965] for the effect of horizontal convergence and divergence on skin temperature so that we can modify the hypothesis of *Marmorino et al.* [2004] to be applicable for all values of the ambient strain.

[15] The skin temperature response to vertical strain from internal waves should be well-approximated by ignoring horizontal variations of the strain field because horizontal scales of internal waves ($\geq$O(10 m)) are much greater than the vertical scale of the cool skin (O(1 mm)) [*Osborne*, 1965]. An important timescale on which the skin-layer adjusts is δ^2/κ, which is about 10 s if δ is assumed to be O(1 mm) [*Osborne*, 1965]. For motions like internal waves, which vary on a timescale much longer than δ^2/κ, the response of the cool-skin can be treated as a static balance (i.e., the time derivative in the heat equation can be ignored). Given these simplifications, the heat equation can be written as

$$\Theta_{zz} = \frac{-\alpha z}{\kappa}\Theta_z, \tag{3}$$

where subscripts indicate derivatives, $\Theta \equiv T(z) - T(-\delta)$ is the deviation from the bulk water temperature, $T(-\delta)$, and the profile of vertical velocity is taken to be linear so that $w = -\alpha z$. The boundary conditions are

$$\Theta(z = -\delta) = 0 \tag{4}$$

$$\Theta_z(z = 0) = \frac{Q}{\rho c_p \kappa}, \tag{5}$$

where Q is the interfacial heat flux (positive downward). *Osborne* [1965] modeled Q as long-wave radiative heat loss from the sea surface, but we shall model Q as a crude bulk formula representation of sensible and latent heat flux, namely $Q = A(T_{air} - T_{skin})$, where T_{air} is an effective air temperature (assumed fixed), T_{skin} is the skin temperature, and A is a constant taken to be 30 W/m^2/°C. (This choice of A gives a heat flux of -90 W/m^2 for an air-sea temperature difference of 3°C.)

[16] After solving the differential equation (equation (3)) and applying the second boundary condition (equation (5)), we find

$$\Theta(z) = \Theta(0) + \frac{Q}{\rho c_p \kappa}\int_0^z e^{\frac{-\alpha\sigma^2}{2\kappa}} d\sigma, \tag{6}$$

where $\Theta(0)$ has arisen as an integration constant and σ is a dummy variable. Application of the first boundary condition (equation (4)) yields

$$\Theta(0) = \frac{Q}{\rho c_p \kappa}\int_{-\delta}^0 e^{\frac{-\alpha z^2}{2\kappa}} dz. \tag{7}$$

Note that when the strain rate, α, is zero, we recover the canonical equation for the cool skin [e.g., *Saunders*, 1967, equation (2)]. Using the expression given above for the surface heat flux, Q, equation (7) can also be expressed as

$$\Theta(0) = \frac{A(T_{air} - T(-\delta))}{\rho c_p \kappa + A\int_{-\delta}^0 e^{\frac{-\alpha z^2}{2\kappa}} dz}\int_{-\delta}^0 e^{\frac{-\alpha z^2}{2\kappa}} dz. \tag{8}$$

Equation (7) (or, equivalently, equation (8)) is an exact solution of equations (3)–(5) specifying the magnitude of the cool-skin effect as a function of the surface strain rate, given the cool-skin thickness, δ. The value of δ is not known a priori and may in fact be a function of α. For constant δ, the bulk-skin temperature difference increases from low values at large, positive strain rates and asymptotes to the air-sea temperature difference at large, negative strain rates (Figure 3a).

[17] Equation (1) differs in some important ways from equation (7). Equation (1) is an exact solution to a system of equations similar to equations (3)–(5), the only difference being that the water-side boundary condition (equation (4)) is applied at $-\infty$ instead of $-\delta$ [*Leighton et al.*, 2003]. This difference in boundary conditions is important, though. The system of equations leading to equation (1) has no solution for negative strain rates (downwelling), and equation (1) is very nearly the same as the asymptotic solution to equations (3)–(5) for large, positive strain rates given by *Osborne* [1965], as was noted by *Marmorino et al.* [2004]. Equation (1) (which we refer to as the "large α solution" in Figure 3a) is a good approximation for large, positive strain rates, but diverges rapidly from equation (7) at strain rates of the order κ/δ^2 (i.e., on the order of $0.05\ s^{-1}$). While equation (7) neglects surface renewal processes and is probably unrealistic in its own right, we find it preferable to equation (1) because it reproduces the expected conductive balance at zero strain and its solution remains finite for all strain rates.

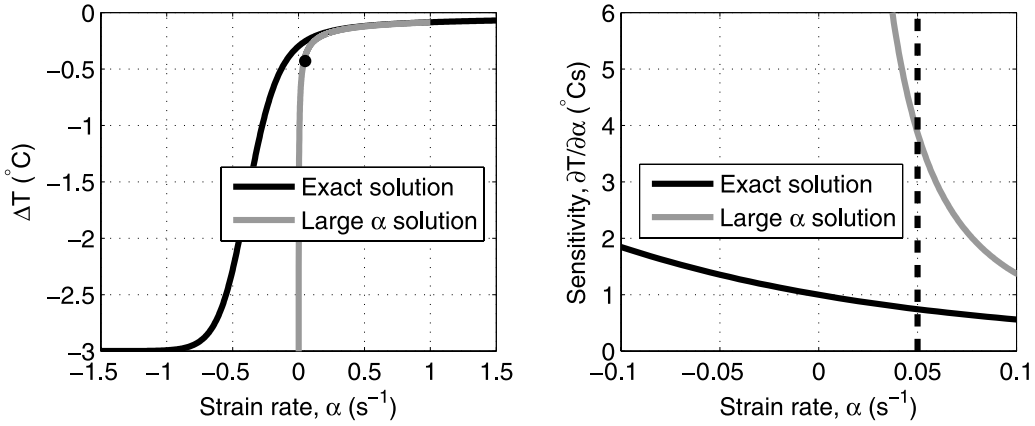

Figure 3. (left) Expected equilibrium dependence of the cool-skin effect on the vertical strain rate, evaluated for δ = 1.5 mm and an air-sea temperature difference of 3°C. (right) Expected sensitivity of the cool-skin effect to variations in the vertical strain rate. In each plot, the solid black line is from equation (7) and the gray line is from equation (1). The ambient strain rate inferred by *Marmorino et al.* [2004] from equation (1) is marked by a black dot in the left plot and by a dashed line in the right plot.

[18] Use of a solution that is invalid for small strain rates has an important effect on the estimated sensitivity to variations in the strain rate in the vicinity of a small ambient strain. Typical strain rates in the upper few meters of the ocean under low-wind conditions are probably smaller in magnitude than ±0.1 s^{-1}; this would correspond to a velocity on the order of 10 cm/s at 1 m depth. The strain-rate sensitivity, $\partial\Theta/\partial\alpha$, of the model for this range of strain values is considerably smaller than the value of 4°C/s^{-1} estimated by *Marmorino et al.* [2004] from equation (1) (Figure 3b). For the parameter values used to evaluate equation (8) in Figure 3 (δ = 1.5 mm, $Q = A(T_{air} - T_{skin}) \approx -80$ W/m^2), the internal-wave strain rate would need to be on the order of ±0.1 s^{-1} to cause a ±0.1°C temperature signal. Such a strain rate is unrealistically large for internal waves; for example, even the energetic nonlinear internal waves observed in the New York Bight are associated with strain rates more than 10 times smaller [*Gasparovic et al.*, 1988; *Liu*, 1988].

[19] Numerous models of the cool skin have been proposed, but, as pointed out by *Castro et al.* [2003], the main difference between the models is in the choice of δ, or for surface renewal models [e.g., *Castro et al.*, 2003, and references therein], in the choice of renewal timescale (which implies a choice of δ). Osborne recognized the choice of a model for δ as a fundamental difficulty of his theory, and considered three different scenarios for the spatio-temporal behavior of δ in response to internal waves. One plausible scenario is that δ, being primarily set by rapid processes related to surface waves and turbulence, is essentially insensitive to the relatively weak variations of strain rate associated with internal waves and can be treated as a constant. By the same reasoning, an unlikely scenario is that the boundary layer's lower edge is advected upward and downward by the internal-wave vertical velocity signal. (*Osborne* [1965] included this scenario for consideration of short-period surface waves.) A third scenario is that surfactants, subject to horizontal convergences and divergences associated with the internal waves, modulate the thickness of δ in space and time by affecting near-surface turbulence; this scenario is distinct from the first two in that we suppose that the surface strain from internal waves is so weak that it has no direct effect on δ or Θ, but has an indirect effect via surfactants.

[20] Very little is known from field measurements about spatial variations in the thickness of the cool skin, much less about the relation of cool-skin thickness to internal waves. Yet, both the magnitude and phase of the cool-skin response to internal waves are expected to depend on this relationship. Of the scenarios described above, the first ($\delta \approx$ constant) and third (δ modulated by surfactant convergence) seem most plausible. For a spatially uniform value of δ, the skin temperature signal should be in phase with the strain-rate signal, and if δ varies in response to the internal-wave straining (second or third scenarios above), the skin temperature signal should be 90° out of phase with the strain-rate signal [*Osborne*, 1965]. Given the O(1 mm) thickness of the cool skin, δ is very difficult to measure in the field and our data yield no direct information on δ. Fortunately, knowledge of the behavior of δ in response to internal waves is not required to evaluate the cool-skin straining hypothesis for a skin temperature signal; detection of an internal-wave signal in the bulk-skin temperature difference would constitute sufficient evidence that internal-wave signals observed in the skin temperature are due to modulation of the cool-skin effect. Our approach to testing this hypothesis is described further in section 2.3.

2.2. Modulation of Warm-Layer Entrainment

[21] During conditions of light winds and strong insolation, heat and momentum are concentrated near the surface in a "diurnal warm layer" [*Stommel and Woodcock*, 1951; *Stommel et al.*, 1969; *Price et al.*, 1986; *Fairall et al.*, 1996b] that can exhibit temperature gradients as large as 4°C/m [e.g., *Walsh et al.*, 1998, and references therein]. The evolution of the warm layer can be modeled accurately by assuming the depth of the layer is governed by a bulk Richardson number that remains on the threshold of criticality; the depth of the layer is then proportional to $I_\tau/\sqrt{I_Q}$

where I_τ and I_Q are the accumulated momentum and heat fluxes applied to the layer [*Fairall et al.*, 1996b].

[22] *Walsh et al.* [1998] observed propagating patterns in infrared skin-temperature measurements from the western Pacific warm pool and made a convincing case that the patterns were associated with oceanic internal waves with periods of 30 min to 2 h. Temperature profiles from a nearby buoy showed that internal waves modulated the depth of the O(1 m)-thick warm layer by O(1 m) [*Walsh et al.*, 1998]. In light of this additional observation, *Walsh et al.* [1998] hypothesized that the observed SST signal was caused by modulation of entrainment at the base of the warm layer.

[23] Within the context of the warm-layer model of *Fairall et al.* [1996b], it stands to reason that modulation of the depth of the warm layer by internal waves should affect the entrainment at the base of the layer. The model requires that the Richardson number remain at the threshold of criticality, i.e.,

$$\frac{D\Delta T}{(\Delta U)^2} = C, \tag{9}$$

where C is a constant (involving the critical Richardson number and physical constants) and ΔT and ΔU are the temperature and velocity differences between the base of the warm layer (depth D) and the surface. Though the *Fairall et al.* [1996b] warm-layer model does not explicitly consider advection, conservation of heat and momentum in the presence of vertical advection requires that ΔT and ΔU are not directly affected by vertical advection. That is, vertical advection does not directly modify the surface properties or the temperature or velocity at base of the warm layer; it merely modifies the depth D over which the temperature and momentum gradients occur. Thus an upward displacement of the base of the warm layer will initially reduce D, reducing the Richardson number below its critical threshold and causing an adjustment of ΔT, ΔU, and D to ensure that (9) is satisfied.

[24] The near-surface mixing signal is irreversible; it is easy to imagine how the phase of the wave with upward advection could produce a cool signal, but it is more difficult to imagine how downward advection of the base of the warm layer could produce a warm signal. *Walsh et al.* [1998] acknowledge this potential difficulty with their hypothesis and point out that one might expect the spatial pattern produced by such a mechanism to vanish after one complete wave cycle. They suggested that a more complex, nonrepeating internal wave field might always have a surface signal. However, it is conceivable that modulation of entrainment at the base of the warm layer, in conjunction with the positive heat fluxes required for the existence of a warm layer, could produce a warm anomaly of similar magnitude to what is observed. If we suppose that entrainment is shut off during the half-cycle that the vertical velocity is downward, the change of temperature expected during that period under the *Fairall et al.* [1996b] model would be

$$\Delta T' = \frac{Q_{WL}\Delta t}{\rho c_p D}, \tag{10}$$

where Δt is the wave period and Q_{WL} is the net heat flux applied to the warm layer. (Note that the factor of two associated with the wave half-cycle is canceled by a factor of two that comes from an assumption of linear stratification within the warm layer in the *Fairall et al.* [1996b] model.) If Q_{WL} has the modest value of 300 W/m^2, the wave period is 1 h, and D = O(1 m), the surface temperature would be expected to warm by 0.26°C, an amount comparable to the warm anomalies observed by *Walsh et al.* [1998] and *Marmorino et al.* [2004]. This order of magnitude calculation lends some plausibility to the idea that entrainment modulation, coupled with the positive surface heat fluxes required for the existence of a warm layer, can produce both warm and cool SST anomalies. In section 5.2, a numerical model is used to provide further support for this idea.

2.3. How Can These Hypotheses Be Tested Using Field Data?

[25] The principal data set used in this paper consists of infrared measurements of SST (i.e., skin temperature) and coincident subsurface temperature measurements nominally spanning depths of 20 cm to 20 m (section 3). We seek to determine whether the cool-skin straining hypothesis advocated by *Marmorino et al.* [2004] or the modulation of warm-layer entrainment hypothesis proposed by *Walsh et al.* [1998] provides a more plausible account of the prominent internal wave SST signal observed under low winds in CBLAST-Low.

[26] The mechanism proposed by *Marmorino et al.* [2004] is purely a cool-skin effect. If a cool-skin straining mechanism is responsible for the internal-wave signal observed in airborne infrared measurements of the skin temperature, we would expect the spatial pattern of the surface temperature signal to be quite similar to the spatial pattern of bulk-skin temperature difference, since the signal is hypothesized to result from variations in the bulk-skin temperature difference. Similarly, if the signal observed in the skin temperature is identical, or very similar, to the signal observed in the bulk fluid (10–30 cm depth), this would indicate that the SST signal results from processes in the bulk fluid and would thus constitute grounds for rejection of the cool-skin straining hypothesis. In addition, under the cool-skin straining hypothesis, the signal would be expected to be present regardless of the presence of a diurnal warm layer, so long as internal waves are present.

[27] The mechanism proposed by *Walsh et al.* [1998] is not a cool-skin effect. If a warm-layer entrainment mechanism similar to the one hypothesized by *Walsh et al.* [1998] is responsible for the internal-wave signal, we would expect spatial or temporal fluctuations in the bulk water temperature (roughly 20 cm depth) to be nearly identical, in both amplitude and phase, to those measured at the surface. By the same logic, we would expect fluctuations in the bulk-skin temperature difference to have no systematic relationship to the fluctuations observed in the skin temperature.

[28] Of course, it is conceivable that both mechanisms contribute to the observed variability. We will consider this possibility by analyzing data during times when no warm layer is present.

3. Data

[29] The data were collected during the August 2003 Intense Observing Period of the CBLAST-Low field pro-

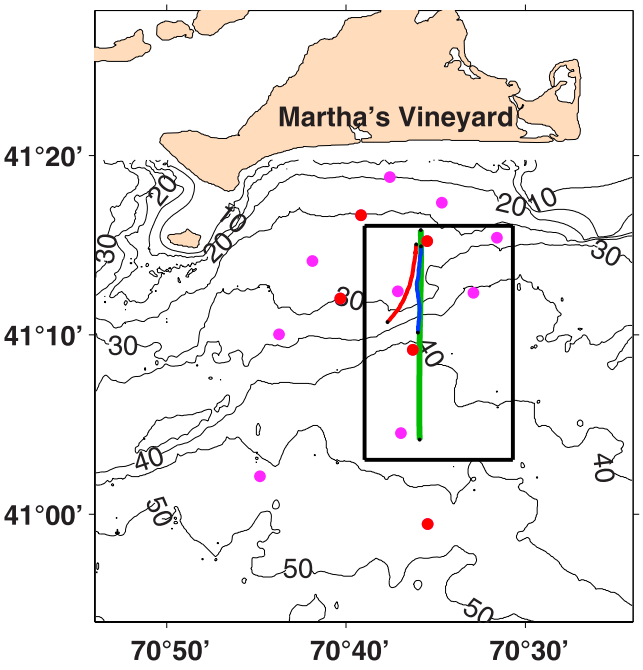

Figure 4. Morning survey section (blue line) and the late-afternoon section (red line) from 15 August 2003. The aircraft survey track is indicated by a green line. Isobaths (black contours) are given in meters. Also shown are the mooring locations for the CBLAST-Low Intense Observing Period of August 2003 (pink and red circles, with red indicating more heavily instrumented moorings).

gram, which took place in the coastal region south of Martha's Vineyard, Massachusetts. Some key observational elements of the field program were an oceanic mesoscale array of 14 moorings (Figure 4), the Air-Sea Interaction Tower (ASIT) [*Edson et al.*, 2007], aircraft surveys, and ship surveys. The field program took place in water depths ranging from 10 to 50 m. The area is characterized by light to moderate winds, the passage of synoptic weather systems, and a strong thermocline during the summer.

[30] Three moorings within the oceanic mesoscale array were instrumented with subsurface vertical temperature/salinity arrays as well as velocity measurements. In situ measurements of precipitation, relative humidity, wind speed and direction, incoming short- and long-wave radiation, and air temperature were also made at these three fixed locations [*Edson et al.*, 2007; K. Colbo and R. A. Weller, The accuracy of the IMET sensor package, submitted to *Journal of Atmospheric and Oceanic Technology*, 2006]. These surface meteorological measurements were used with the TOGA-COARE bulk flux algorithm [*Fairall et al.*, 1996a, 2003] to estimate the air-sea fluxes of heat, momentum, and moisture.

[31] Shipboard operations were conducted from the FV *Nobska*. A bow-mast on the *Nobska* was equipped with upward and downward looking Heitronics model KT-19.82 infrared radiometers (8–14 μm) to accurately measure the ocean skin temperature (corrected for sky reflection) at a 1 Hz sampling frequency. The KT-19 was calibrated in the laboratory, but owing to a temperature dependence in the response of the instrument, the resulting SST showed a warm bias. We estimated the magnitude of this bias by comparing the shallowest subsurface temperature measurement (~30 cm) to the SST during nighttime conditions when a net heat loss from the ocean surface leads to a well-mixed surface layer with a cool skin. This comparison suggested the estimated SST was at least 0.5°C too warm. The estimated bias is calculated at the time of minimum heat loss during the nighttime, when the cool skin effect is expected to be minimal. Any residual bias is within the expected accuracy of the system in laboratory conditions, but it is worth noting that the conclusions of this paper are not affected by radiometer bias since the hypotheses are evaluated by comparison of fluctuations in the bulk and skin temperature.

[32] Subsurface temperature measurements were collected from the *Nobska* using 21 Seabird SBE 37's and SBE 39's sampled at 4 or 5 seconds. The instruments were towed from the *Nobska*'s boom crane, and care was taken to ensure that the instrument chain was as far as possible to the side of the vessel's wake. The towed instrument chain could be deployed with vertical spacing greater than or equal to 0.5 m. The horizontal distance between samples depends on the vessel's speed (5–7 kts) and the sampling rate (0.2–1 Hz); the nominal horizontal separation between SST measurements was 2 m and the separation between sequential subsurface measurements was about 8 m. Three of the subsurface instruments measured pressure, and these pressure measurements were used to estimate the sensor depths as described in the appendix. Aliasing of surface waves is a concern, but for the low-wind conditions under consideration here, the seas were calm and surface wave activity was minimal.

[33] Airborne infrared measurements were made using the University of Washington Applied Physics Laboratory's Infrared System (APLIS). APLIS consists of two sensor pairs that include a high-resolution, low-noise AIM model 640Q longwave (8–10 or 8–9.5 μm) IR camera (512 × 640 pixels) and a calibrated Heitronics model KT-15.82 narrow field-of-view radiometer (9.6–11.5 μm). One sensor pair is directed near-nadir to measure sea surface radiance and the other is directed upward to measure sky radiance. This combination of sensors provides high-resolution, low-noise imagery of calibrated, sky-corrected sea surface temperature. In addition to providing high resolution, the longwave cameras can be used during the day with minimal contamination due to reflected sunlight. Images were acquired at 1 Hz in order to provide an instantaneous 2-D map of surface temperature with a thermal resolution of roughly 0.02°C. For the nominal altitude of 875 m in 2003, the spatial resolution was better than 0.9 m. A down-looking Pulnix digital video camera was implemented to supplement the IR measurements and to characterize the sea surface condition. During the 2003 CBLAST-Low experiments, APLIS was deployed aboard a Cessna Skymaster aircraft operated by Ambroult Aviation (Chatham, MA).

[34] We have identified a useful case study of enhanced SST variability in low winds utilizing ship, mooring, and aircraft data from 15 August 2003. Winds were low-to-moderate throughout the day, with wind speeds of 2.5–4.5 m/s in the early morning hours decreasing to speeds of 1–2 m/s by about noon local time. We carried out nearly

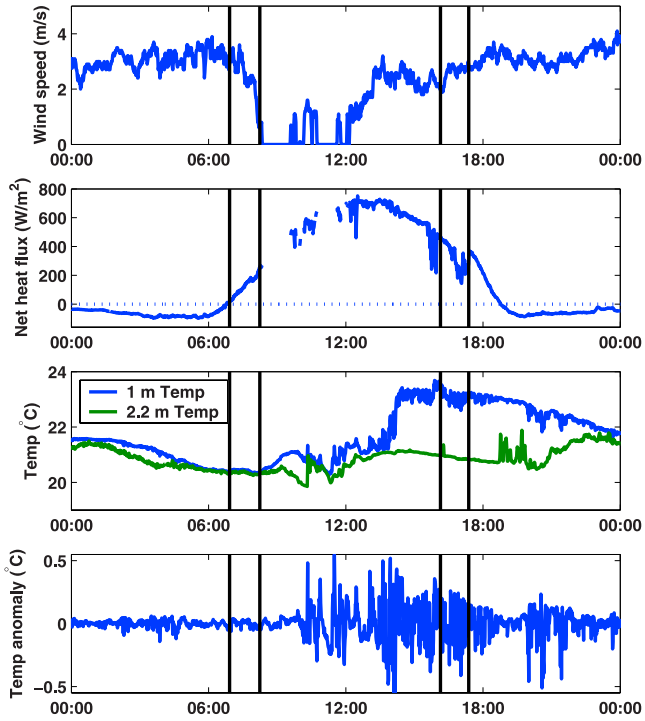

Figure 5. Data from a surface buoy near the termination point of the two transects. The time of each transect is marked by a pair of vertical black lines. (first plot) Wind speed. (second plot) Net heat flux into the ocean. (third plot) Subsurface temperature at the 1-m and 2.2-m levels (blue and green lines, respectively). (fourth plot) Temperature anomaly at 1 m depth relative to a 1-hour running average.

overlapping ship transects (Figure 4), one around 7:30 and another around 16:30 (local time). During both surveys, coincident radiometric SST measurements and subsurface temperature and salinity measurements were collected. Both sections were about 10 km long in a cross-shore direction and spanned water depths of about 22–37 m. Each transect took about 70 min to complete. The mean wind speeds and surface turbulent heat fluxes were very similar during the two transects, but the low winds and strong daytime heating led to the development of strong, shallow temperature stratification, with a temperature gradient of about 2°C over the upper 2 m. This strong temperature gradient and the thickness of the warm layer are roughly consistent with the scaling analysis of *Price et al.* [1986]. During the afternoon survey, the Cessna Skymaster flew almost directly over the *FV Nobska* along a similar track (Figure 4). The shipboard infrared SST measurements indicated that the 100- to 2000-m SST variability was much larger during the afternoon survey. We have chosen to focus on this case study because it will allow a more direct evaluation of the cool-skin straining and warm-layer entrainment hypotheses than has been possible with previous data sets. In addition, this directly addresses a central CBLAST-Low goal of understanding SST and boundary layer variability under low winds.

[35] Unless otherwise specified, all times are local (i.e., Eastern Daylight Saving Time, equal to UTC minus four hours), and all smoothing and bandpass filtering is carried out using a moving-average filter. We use the oceanographic convention in stating surface heat fluxes: negative surface fluxes cool the ocean.

4. Results

4.1. Observed Subsurface Expression of Low-Wind SST Variability From F/V *Nobska*

[36] The evolution of wind speed, surface heat flux, and near surface thermal structure on 15 August 2003 are summarized in Figure 5 using data from a nearby buoy. The pairs of vertical black lines mark the times of the two survey sections that are discussed here. The wind speed was low-to-moderate throughout the day, only exceeding 3 m/s for several hours up to 07:30 (local) and after 18:00 (local). The moderate wind speeds of the early morning hours and nighttime cooling of the sea surface facilitated the formation of a well-mixed surface layer as is indicated by the small temperature difference between the 1 m and 2.2 m levels. Around 08:30 (local), the wind speed dropped below the detection threshold of the anemometer, and near surface thermal stratification increased rapidly. As the near surface stratification increased, so did the variability in 1 m temperature (Figure 5, bottom). The temperature difference between the 1 m and 2.2 m levels was about 2°C for much of the afternoon, so perhaps it should not be surprising that the temperature variability should be relatively large in the presence of such an extreme temperature gradient.

[37] The rapid warming of the sea surface during the day is reflected in the difference of SST observed in the morning and afternoon surveys, which exceeded 2.5°C at most locations along the track. Figure 6 shows the observed SST along the two survey tracks and the corresponding temperature anomalies relative to a 1 km running average. The subkilometer-scale variability in SST was significantly larger during the afternoon survey.

[38] A cool skin is expected to have been present during both transects. Measurements from the buoys near the endpoints of the ship transects indicate that the surface heat fluxes were similar during the morning and afternoon surveys. For example, the combined latent, sensible, and long-wave heat loss from the sea surface at the buoy nearest the southern end of the two transects averaged -108 W/m^2 during the morning survey and -111 W/m^2 during the afternoon survey. Although the average net solar radiation was nearly twice as large during the afternoon survey (388 versus 203 W/m^2), the solar heating was not large enough to negate the cool-skin effect. Assuming that roughly 6.7% of the net solar radiation is absorbed within the skin layer [*Wick et al.*, 2005], the average net surface heat loss from the skin layer was -94 W/m^2 during the morning survey and -85 W/m^2 during the afternoon survey. Since the wind speeds were also comparable and most models of the cool skin depend only on wind stress and heat flux, the magnitude of the cool-skin effect is expected to have been comparable during the two surveys. For example, the *Fairall et al.* [1996b] model suggests that the cool-skin temperature difference was within 0.01° of 0.37°C during both surveys.

[39] The near-surface stratification was relatively weak during the morning survey, and the variability in near surface temperature was small (Figure 7, top). A strong

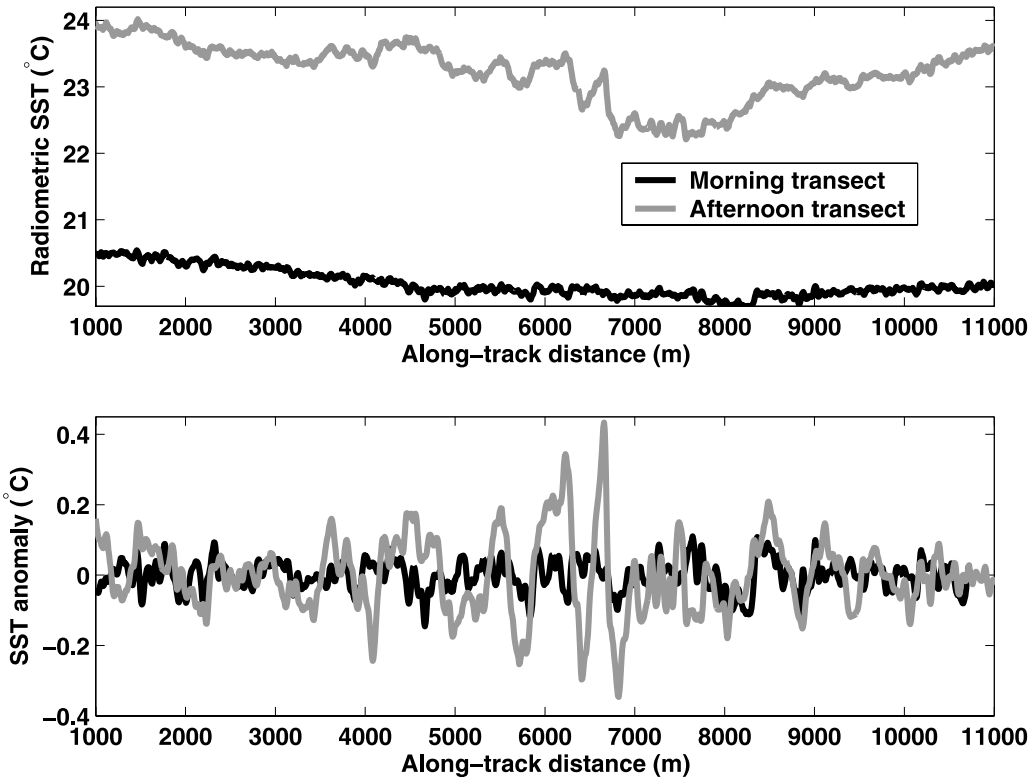

Figure 6. (top) Radiometric SST observed along the morning and afternoon survey tracks. (bottom) SST anomaly relative to a 1-km running average. The subkilometer-scale spatial variability in SST was considerably larger during the afternoon transect. The along-track distance increases moving onshore from south to north.

vertical temperature gradient of O(1°C m^{-1}) was present at 5–15 m depth, and this thermocline deepened and weakened toward the coast. Above this thermocline, surface and subsurface temperature fluctuations were modest during the morning survey. Quasiperiodic isothermal excursions were observed in the main thermocline along the entire track; these fluctuations are associated with vertical displacements of isotherms by the oceanic internal wave field.

[40] The surface and subsurface thermal structure observed during the morning survey can be contrasted with that observed during the afternoon survey (Figure 7, bottom). The thermal structure in and below the main thermocline remained relatively similar to that seen during the morning survey. However, over the course of the day, a substantial temperature gradient had developed just below the surface, having a value of 0.5–1°C m^{-1} on the upper meter over much of the section. This very shallow thermocline, located in the upper few meters of the water column, is comparable in strength to that of the main thermocline. One (somewhat arbitrary) way of defining the depth of the diurnal warm layer is as the depth where the temperature is 1°C less than the SST. Alternatively, this depth may be thought of as a measure of the near-surface stratification. Under this definition, the depth of the warm layer was almost exclusively less than 4 m and was less than 1 m at along-track coordinates of 5000–6600 m. The strong, shallow stratification allows substantial temperature anomalies to exist near the surface in association with vertical advection by the internal-wave field.

[41] Given only temperature transects, it is not possible to prove conclusively that horizontal variations in the subsurface temperature at small scales (i.e., smaller than a baroclinic deformation radius) are due to internal waves. However, it should be noted that, so long as the temperature fluctuations are not compensated by salinity variations so as to give no horizontal variation in density and pressure, the fluctuations should be associated with internal waves since horizontal pressure variations on scales less than the deformation radius (about 3 km in this case) are not expected to be in a steady-state balance. That is, small-scale pressure variations are expected to be balanced by velocity fluctuations, analogous to the way that variations in sea surface height at scales of tens of meters seen in a photograph are expected to be surface waves. Thus, when the subsurface temperature data are high-pass filtered along the survey track to remove the large-scale temperature variations, the resulting temperature anomalies are expected to primarily represent horizontal variations in temperature associated with vertical displacements by the internal-wave field.

[42] The along-track temperature anomalies from the two surveys are shown in Figure 8. These temperature anomalies were computed by band-passing the along-track temperature data at 50–1000 m scales. During the morning survey, temperature anomalies were relatively small above the main thermocline (located at 5–15 m depth), typically less than

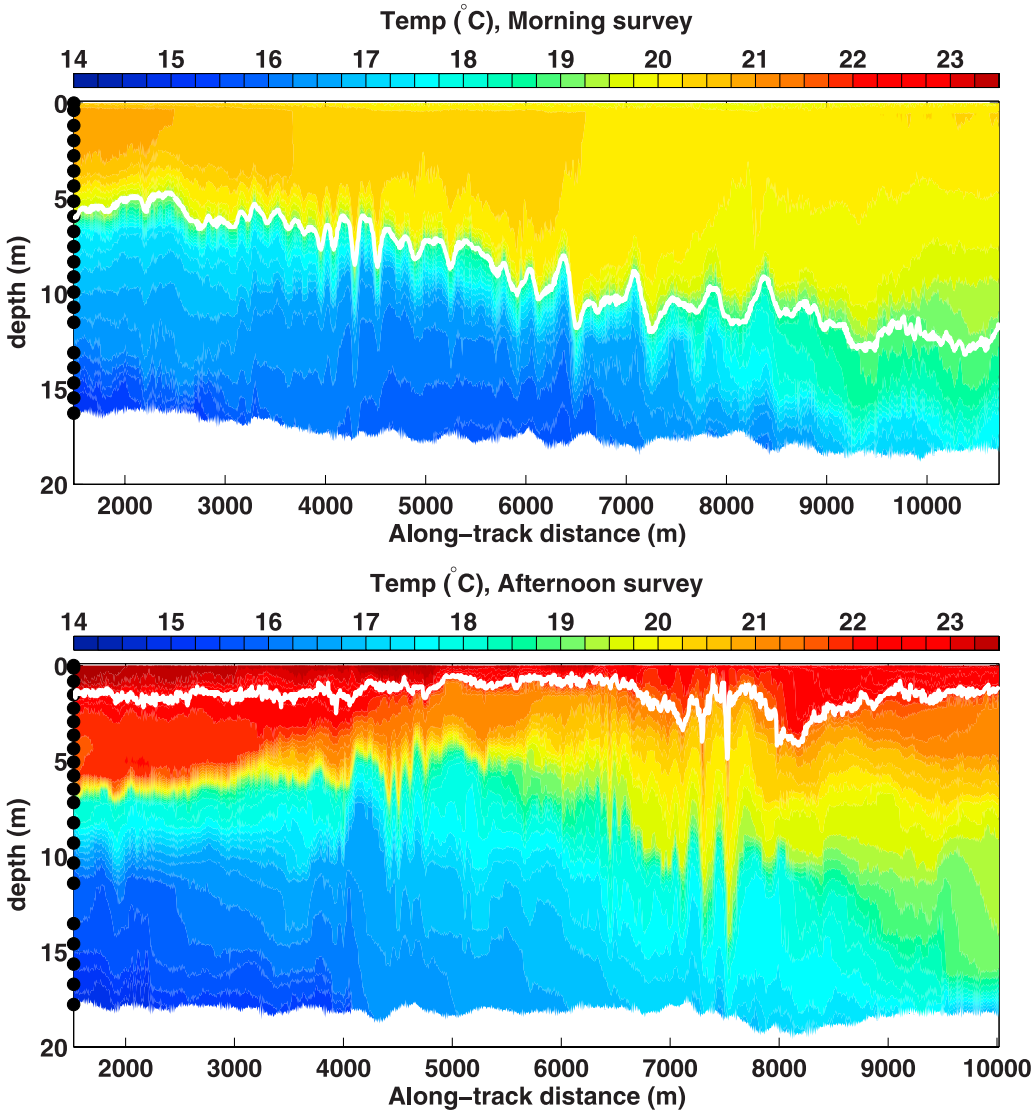

Figure 7. Temperature data from the (top) morning survey section and (bottom) afternoon section. The black dots on the left edge of each plot mark the nominal instrument depths, and the thick white line marks the depth where the temperature is 1°C less than the SST. The along-track distance increases moving onshore from south to north.

0.05°C. In contrast, the afternoon survey shows strong temperature anomalies in the upper few meters, coherent with fluctuations at greater depths. Although not all of the band-passed temperature signal should be ascribed to internal waves, the subsurface temperature anomalies are, for the most part, vertically coherent as is expected for internal waves.

[43] To examine variability at smaller scales and to clarify the relationship between surface and subsurface temperature fluctuations, the temperature data from the afternoon survey were band-pass filtered at 90–500 m scales. Examination of the surface and subsurface temperature signals at these scales suggests that most of the SST signal during the afternoon survey is associated with variations in the bulk temperature (Figure 9), since the SST signal closely resembles the temperature signal at 20 cm depth. In other words, there is no evidence that the dominant variations in skin temperature at these scales are associated with variations in the bulk-skin temperature difference. The largest signal in band-passed SST and 20 cm temperature occurs at along-track coordinates of 5500–7000 m. This region exhibited the strongest near-surface stratification and a complex vertical structure in subsurface temperature fluctuations.

[44] Although description of the internal-wave field in the study region in terms of vertical normal modes is probably quantitatively inappropriate because of the relatively strong, vertically sheared tidal flow [*Pritchard and Weller*, 2005] and spatial variations in bathymetry and stratification, there is some evidence that the large variations in surface temperature at along-track coordinates of 5500–7000 m are associated with waves resembling the second baroclinic mode. For example, the temperature measured at the shallowest subsurface sensor in this region is roughly out of phase with that measured near 14 m depth. This phase

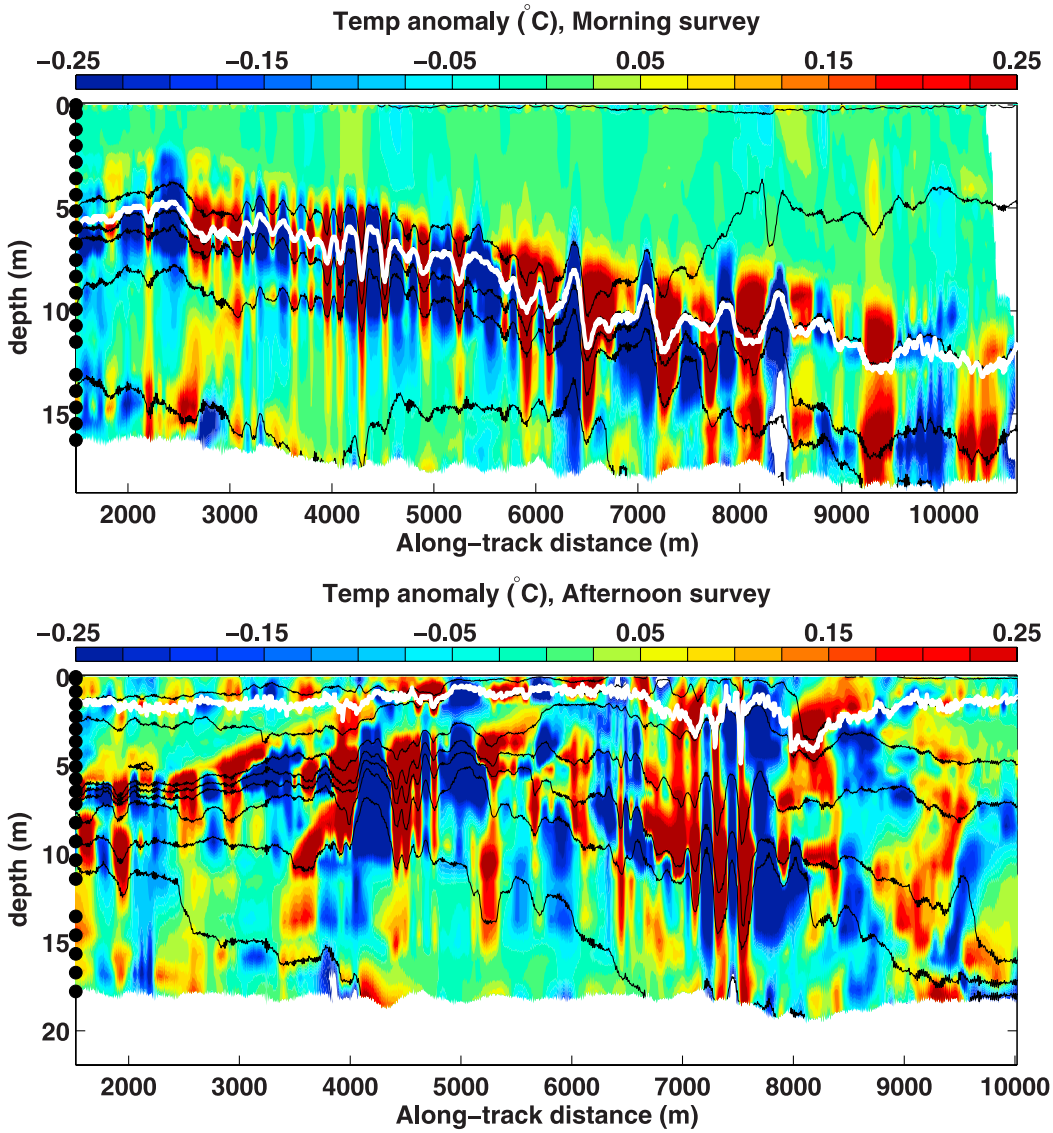

Figure 8. Temperature anomaly along the (top) morning survey section and (bottom) afternoon section. The anomalies are computed by band-passing the temperature at 50- to 1000-m scales. The black dots on the left edge of each plot mark the nominal instrument depths. The black lines mark isotherms at 1°C intervals, and the thick white line marks the depth where the temperature is 1°C less than the SST.

relationship, and its significance, were quantified using a Fourier coherence computation over the 4500–7000 m along-track coordinates. The temperature measured at the shallowest sensor is coherent with that measured near 14 m in the 263–556 m wavelength band at 95% confidence (coherence amplitude is 0.68 and level of no significance at 95% confidence is estimated to be 0.596), and the phase angle is about 150°. Although only about half of the 263–556 m variance of the near-surface temperature can be "explained" by temperature fluctuations at 14 m depth, the coherence phase suggests that the largest SST signal may be associated with the second baroclinic mode. This interpretation would make sense if the mechanism for the surface signal involves vertical advection of the base of the warm layer, since computation of the normal mode profiles of vertical velocity indicates that the 2nd mode should have a local maximum in vertical velocity near the warm-layer base. However, this interpretation is questionable because it is not obvious that the antiphased relationship between the two depths is caused by a sign change in the profile of vertical velocity. There may be other reasons for the observed antiphasing of the shallow and deep temperature signals. The evidence that the antiphased temperature fluctuations are associated with a 2nd mode disturbance would be stronger if the temperature data were corroborated by well-resolved velocity profiles, for example.

[45] Evidence for surface temperature signals associated with waves resembling the first baroclinic mode is less ambiguous. Taking the wave packet observed near the 7000- to 7500-m along-track coordinate as an example (visible in Figures 7–9), there is a clear SST signal associated with the wave packet. The SST observed over this wave packet closely tracks the temperature measured near 18 cm depth, and, assuming there is no warm bias in

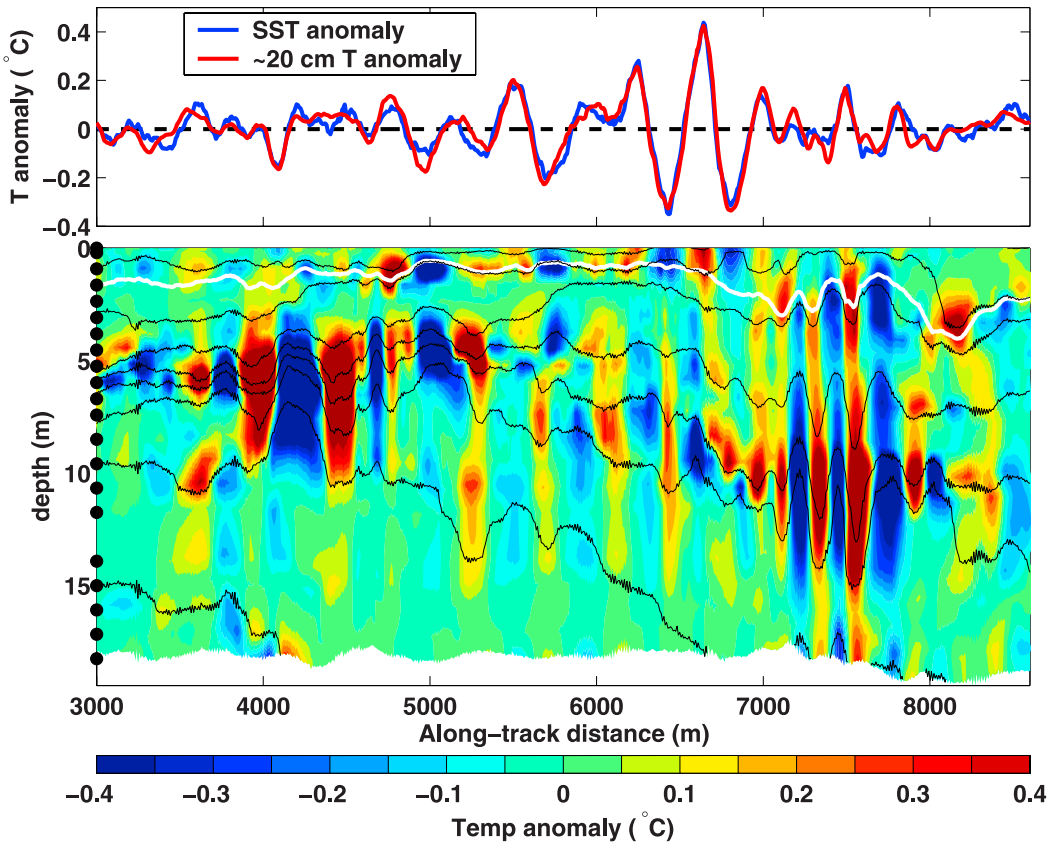

Figure 9. The 90- to 500-m along-track band-passed temperature during the afternoon survey. (top) Signal in SST and the shallowest subsurface temperature measurement (mean depth of 20 cm during the interval shown). (bottom) Signal in subsurface temperature. The black dots on the left edge of the figure mark the nominal measurement depths. The black lines mark isotherms at 1°C intervals, and the thick white line marks the depth where the temperature is 1°C less than the SST.

the SST measurement, the near-surface stratification exceeds 1°C/m on the upper 18 cm (Figure 10). The temperature data (Figure 10) and the along-track filtered data (Figure 11) show that the temperature signal at 18 cm depth is associated with the internal-wave packet. For three of the four wave cycles shown in Figures 10 and 11, the SST signal is very similar to the signal observed at near 18 cm depth (Figure 11). Given the similarity in the isothermal depressions observed near along-track coordinates of 7300 m and 7500 m, the vertical strain-rate signal associated with the two depressions was probably comparable; yet, the SST signals are dissimilar, giving further evidence that cool-skin straining hypothesis cannot account for the SST signal.

[46] Similar relationships between surface and subsurface temperature fluctuations were observed down to the smallest scales that the instruments aboard the *Nobska* could reliably resolve (about 75 m, which corresponds to about 9 samples). An example of such small-scale variability is shown in Figure 12. This particular example comes from the region where the warm layer was shallowest and where the largest temperature signals were found (having horizontal scales of several hundred meters; see Figure 9). The scale of these features (about 75–100 m) is comparable to the features seen in the raw aircraft infrared imagery in Figure 2 and the internal-wave signal can be seen to extend coherently from depth to the surface.

[47] It is perhaps noteworthy that the signal near the surface (upper 20 cm) is not always clearly related to that at depth; for example, there is some near-surface temperature variability at along-track coordinates of 6450–6575 m in Figure 12 that is apparently unrelated to that at greater depths.

4.2. Internal-Wave Signals as Seen in Aircraft and Moored Measurements in Low-Wind Conditions

[48] Aircraft surveys quantified the horizontal variability of SST in the CBLAST-Low study region. Real-time display of SST data on the Cessna and the FV *Nobska* indicated that the 10 to −2000-m SST variability was unusually large during the low-wind conditions of 15 August. Ship and aircraft teams, communicating by radio, then devised a strategy to optimally utilize the ship, aircraft, and moorings to better characterize and understand this low-wind SST variability through overlapping surveys (Figure 4). (The *Nobska* changed course to align with the morning survey section and the aircraft's flight pattern, which partially explains the curvature of the *Nobska*'s track during the afternoon survey.) While the drastic difference in the speed of the aircraft and the ship precludes direct comparison of

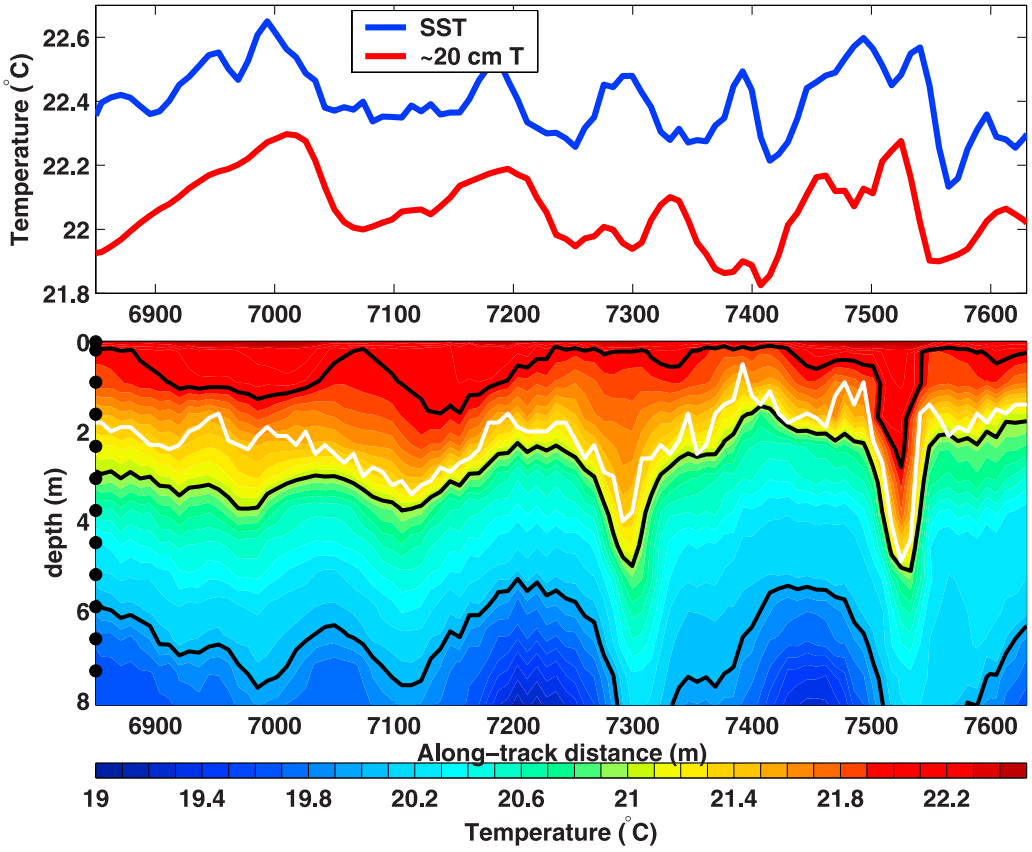

Figure 10. Temperature during the afternoon survey. (top) SST and the shallowest subsurface temperature measurement (mean depth of 18 cm during the interval shown). (bottom) Subsurface temperature. The black dots on the left edge of the figure mark the mean measurement depths for the part of the survey shown. The black lines mark isotherms at 1°C intervals, and the thick white line marks the depth where the temperature is 1°C less than the SST.

the measurements made on the two platforms, the internal-wave signal in the aircraft measurements can be compared with the internal-wave characteristics inferred from the moored measurements of temperature and velocity.

[49] Because of the speed of the aircraft and the infrared imagers aboard the aircraft, the aircraft observations of SST allow a better description of the spatial variability of SST than is possible from the shipboard observations. Successive 444 m × 555 m images of SST can be patched together to form an along-track swath of 444 m width (Figure 13). In constructing this swath, we ignored the gradual deviations of the aircraft's flight track from a due-north straight line. (As can be seen in Figure 4, the aircraft flew in a nearly straight line, and the maximum deviation from the mean longitude did not exceed 90 m over the 20 km track.) We also ignored the subtle image distortion associated with the look-angle of the imager. The SST swath observed on the afternoon of 15 August 2003 reveals the presence of wavelike SST variations at a variety of scales. When inspecting the entire swath, the wavelike features that are most apparent have an along-track length scale on the order of 1 km with crests oriented toward the northeast.

[50] Features with scales of O(100 m) are also apparent, as can be seen in Figure 2, which shows a close-up on part of the image shown in Figure 13 from the vicinity of the mooring near the northern end of the swath.

[51] Additional evidence that the wavelike signal observed in SST is in fact due to internal waves comes from analysis of data from the nearby moorings. The mooring data indicated the presence of quasilinear internal waves with a period of about 45 min during the time of the aircraft overpass (Figure 14). The temperature signal of these internal waves is comparable in size to that observed from the FV *Nobska*. For such high-frequency internal waves, the Earth's rotation can be neglected, so the horizontal velocity signal of the wave is expected to be rectilinear and normal to the wave crests (i.e., the acceleration should be down the pressure gradient). The 20- to 60-min band-passed velocity vectors are roughly rectilinear and normal to the crests and troughs seen in the band-pass filtered SST imagery (Figure 15), suggesting that the 45-min period internal waves may be responsible for the wavelike signal observed in SST. This evidence is less direct than the coincident surface-subsurface observations from the FV *Nobska*, but taken with the ship observations showing a close link between skin temperature fluctuations and subsurface temperature fluctuations due to internal waves, we believe it is a sound inference that the regular pattern of skin temperature

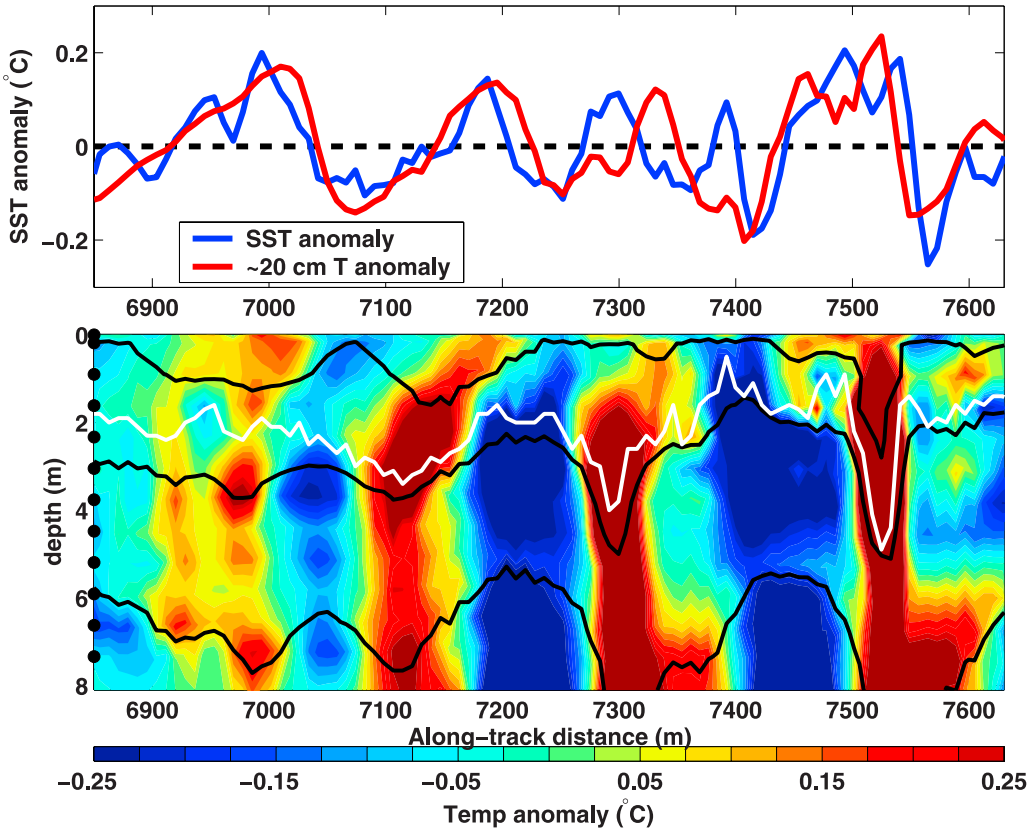

Figure 11. The 20- to 250-m along-track band-passed temperature during the afternoon survey. (top) Signal in SST and the shallowest subsurface temperature measurement (mean depth of 18 cm during the interval shown). (bottom) Signal in subsurface temperature. The black dots on the left edge of the figure mark the mean measurement depths for the part of the survey shown. The black lines mark isotherms at 1°C intervals, and the white line marks the depth where the temperature is 1°C less than the SST.

variability seen in the aircraft IR imagery is associated with the internal waves observed at the moorings.

[52] It would be desirable to obtain an independent estimate of the wavelength of the internal waves observed at the mooring site. If mean flow effects could be neglected and the internal wave dynamics were linear and hydrostatic, it would be possible, in principle, to accurately estimate the wavelength and propagation direction of the waves by examining the transfer function between velocity and dynamic height fluctuations. Assuming linear dynamics might be justifiable and waves with horizontal wavelengths longer than about 100 m should be essentially hydrostatic, but the tidal flow in the region [*Pritchard and Weller*, 2005] is likely to cause substantial Doppler shifting of the internal waves. Lacking knowledge of the intrinsic frequency of the waves, an estimate of the wavelength from the mooring data by such a spectral technique would likely have large errors. The relative error in a transfer function estimate of the wave number vector is expected to be given by the ratio of the frequency Doppler shift to the observed frequency. A worst-case estimate (assuming the wave number is aligned with the mean flow) suggests that the error in such an estimate could exceed 60%. We estimated the wave number by a transfer function approach and obtained wavelengths and orientations comparable to those seen in SST, but we will not report the details of those calculations here because of the large uncertainty in the estimate. The estimate of the propagation direction in the previous paragraph is insensitive to Doppler shifting by the mean flow.

5. Discussion

5.1. Evaluation of Hypotheses

[53] The coincident surface-subsurface shipboard observations and the relationship between the airborne observations of spatially regular SST fluctuations and the internal-wave signals in the mooring data suggest that the observed SST fluctuations are associated with oceanic internal gravity waves. The internal-wave field found during the morning ship survey was similar to that seen in the afternoon survey (e.g., in the vertical displacement of the main thermocline), yet the SST signal was much larger in the afternoon survey.

[54] The fact that the fluctuations in SST observed from the FV *Nobska* closely mimic those observed in the near-surface bulk temperature (Figure 9) strongly suggests that the organized SST fluctuations observed from both the ship and aircraft are not due to modulation of the cool-skin effect by surface straining from internal waves.

[55] The data presented here are consistent with the hypothesis of *Walsh et al.* [1998] that vertical advection by internal waves modulates vertical mixing within the

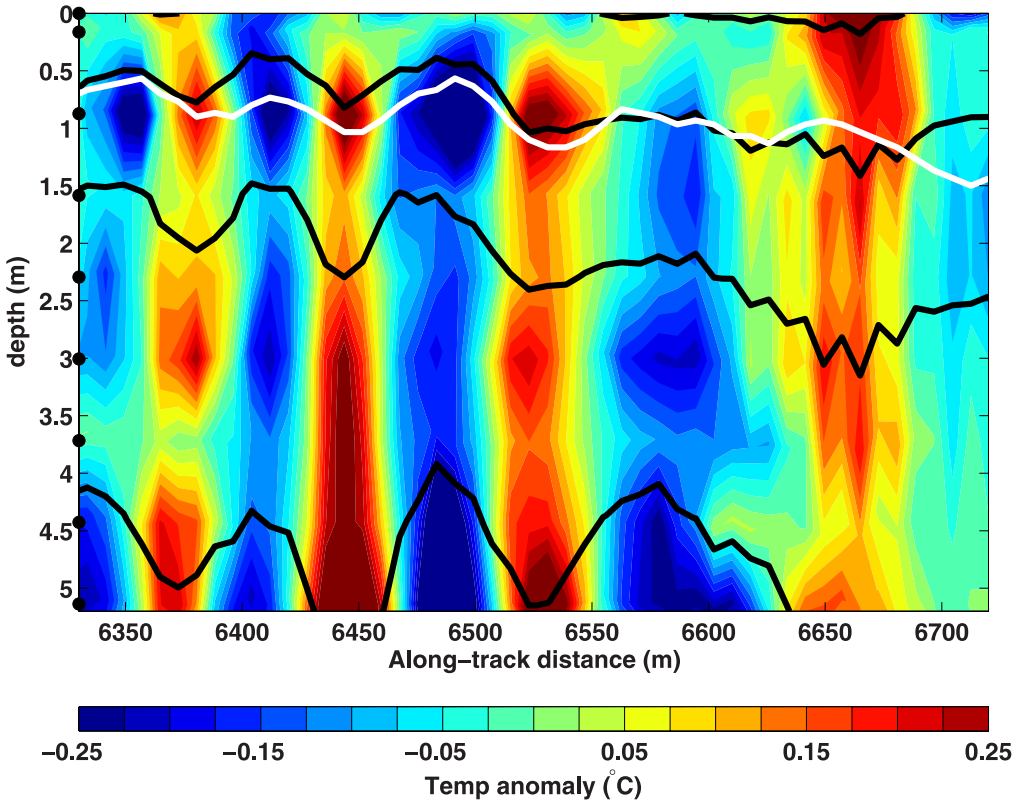

Figure 12. The 150-m along-track high-passed temperature during the afternoon survey, showing that vertically coherent temperature variability was detected down to the smallest scales that could be reliably resolved by the shipboard instrumentation. The black dots on the left edge of the figure mark the mean measurement depths for the part of the survey shown. The black lines mark isotherms at 1°C intervals, and the white line marks the depth where the temperature is 1°C less than the SST.

strongly stratified warm layer that forms under conditions of strong insolation and low winds, but the present data do not allow any direct estimate of the role of vertical mixing in modulating the surface temperature (and do not even give direct evidence that the internal waves modulate near-surface mixing). Internal-wave theory suggests that some diabatic process is required for internal waves to produce an SST signal, and the *Walsh et al.* [1998] mechanism is a plausible explanation of modulation of vertical mixing. Below, the plausibility of the *Walsh et al.* [1998] hypothesis as an explanation for the observed SST variability is investigated further using a numerical model.

5.2. A Numerical Thought Experiment to Further Test the Warm-Layer Hypothesis

[56] A potentially problematic aspect of the warm-layer hypothesis raised by both *Walsh et al.* [1998] and *Marmorino et al.* [2004] is that it is not obvious that modulation of near-surface mixing by internal waves could produce warm SST anomalies, since vertical mixing can only cool the surface (assuming typical thermal stratifications). The order of magnitude calculation given in section 2.2 (equation (10)) suggests that, if vertical mixing across the warm-layer base were shut off during half of the wave cycle, the warm-layer mechanism might produce warm surface temperature anomalies similar to those observed because of the substantial surface heating that is required for the existence of a warm layer. Although the calculation suggests that modulation of warm-layer entrainment is a plausible mechanism for the SST signal, the lack of understanding of the quantitative details of the near-surface mixing in the presence of internal waves, wind-driven vertical shear, solar heating, and surface turbulent heat loss makes the calculation subject to considerable uncertainty. For example, is it reasonable to suppose that vertical advection by internal waves would shut off vertical mixing at the warm-layer base?

[57] To more quantitatively evaluate the plausibility of the warm-layer mechanism proposed by *Walsh et al.* [1998] as an explanation of the observed SST signal, we carried out a numerical "thought experiment" using the upper ocean model of *Price et al.* [1986] with an imposed vertical velocity signal meant to mimic that of an internal wave. The goal of this exercise was to determine whether the vertical heaving of the warm-layer base by internal waves could modulate vertical mixing in a manner sufficient to produce surface temperature anomalies similar to those observed during CBLAST-Low. The *Price et al.* [1986] model is an appropriate tool for such an exercise because it is used as the conceptual basis for some simpler models of the diurnal warm-layer effect [*Fairall et al.*, 1996b; *Schiller and Godfrey*, 2005] and has proven reasonably successful at simulation of the diurnal cycle and warm layer [e.g., *Anderson et al.*, 1996].

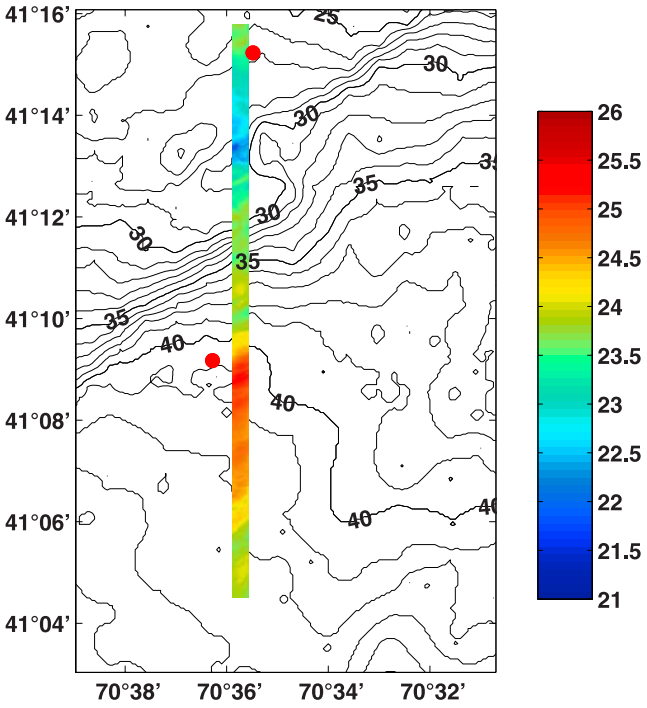

Figure 13. Airborne SST (°C). The axes correspond to the black box in Figure 4. The solid red circles mark the locations of air-sea interaction moorings.

[58] A realistic vertical velocity profile was estimated using normal mode theory and the temperature and salinity profiles observed at one of the moorings during the afternoon of 15 August 2003, the day of the ship and aircraft data presented here. The vertical velocity profiles of the first several modes are all roughly linear in depth over the upper few meters, so the particular modal profile chosen is expected to be less important than the value of the vertical velocity at the warm-layer base. We used the second baroclinic mode and gave it a peak vertical velocity of 1.8 mm/s at 21 m depth and a period of 1 hour. At a depth of 2 m (the nominal base of the simulated warm layer), the amplitude of the fluctuating vertical velocity was about 0.6 mm/s. (This corresponds to a surface strain rate of about 3×10^{-4} s^{-1}, about 30 times smaller than the value chosen by *Marmorino et al.* [2004] to explain the SST signal they observed.)

[59] Dynamical consistency would require also imposing the horizontal velocity signal of the internal wave, but this would complicate the thought experiment and require a systematic consideration of different orientations of the vertically sheared horizontal velocity profile of the internal waves to the wind forcing. Because the profile of horizontal velocity is vertically sheared and reaches a local maximum at the surface, it might be expected to also contribute to modulation of near-surface vertical mixing. Since the goal of this thought experiment is to examine the effect of the vertical velocity on vertical mixing by modulating the Richardson number within the warm layer, we have decided to forgo consideration of the role of the horizontal velocity profile of internal waves.

[60] We initialized the model using a temporally smoothed version of the temperature and salinity observed at one of the moorings and forced the model at 1 min intervals with the heat, freshwater, and momentum fluxes inferred from the buoy meteorological measurements. To ensure adequate simulation of the shallow diurnal warm layer, the vertical resolution was set to 10 cm. The model integration started at midnight on 13 August 2003, about two days before the observations discussed here.

[61] On 15 August 2003, the simulation developed a strongly stratified warm layer by about noon, and the layer deepened steadily throughout the afternoon as the shallow layer continued to accumulate momentum from the wind (Figure 16). The appearance of discontinuities in isotherm depths near the warm-layer base on the shoaling phase of the wave indicates that the vertical velocity signal modulated mixing in the model in a sense consistent with the heuristic argument given in the context of Equation 9 (section 2). Relative maxima in surface temperature occur over the wave troughs, similar to what is observed (e.g., Figure 10), indicating that modulation of near-surface mixing, combined with the surface heating required for formation of a warm layer, is sufficient to produce both warm and cool SST anomalies associated with internal waves. The simulated SST signal is sporadically absent (e.g., the wave cycle just before 15:00 and the one at 18:00) which is reminiscent of the imperfect relation observed between SST and subsurface internal wave temperature fluctuations (e.g., Figure 10).

[62] The fact that an appreciable signal in SST (up to about ±0.08°C) is produced by a modest modulation of the depth of the warm-layer base (<1 m) suggests that the *Walsh et al.* [1998] mechanism is a plausible explanation of the observed SST signal. For comparison, the surface strain rate imposed in the model can be used to estimate the SST signal expected from modulation of the cool-skin effect. Using the surface strain rate of 3×10^{-4} s^{-1}, the observed bulk heat fluxes, and the cool-skin thickness predicted by the *Fairall et al.* [1996b] cool-skin model ($\delta \approx 1.7$ mm), evaluation of equations (7) and (2) suggests that modulation of the cool-skin effect might produce an SST signal of 0.0002 to 0.0012°C, where the range of values allows for the possibility that the ambient strain rate might be between ±0.1 s^{-1}.

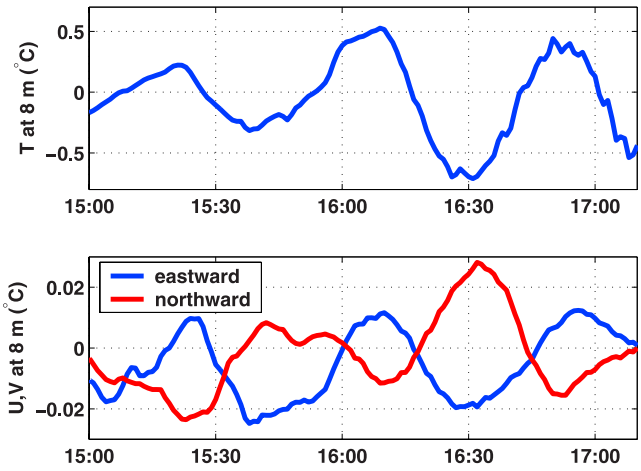

Figure 14. (top) Internal-wave temperature and (bottom) velocity signals from a VMCM at 8 m depth at the southern mooring depicted in Figure 13; the data have been filtered to pass variability in the 11- to 65-min period band. The SST swath in Figure 13 was sampled around 16:30.

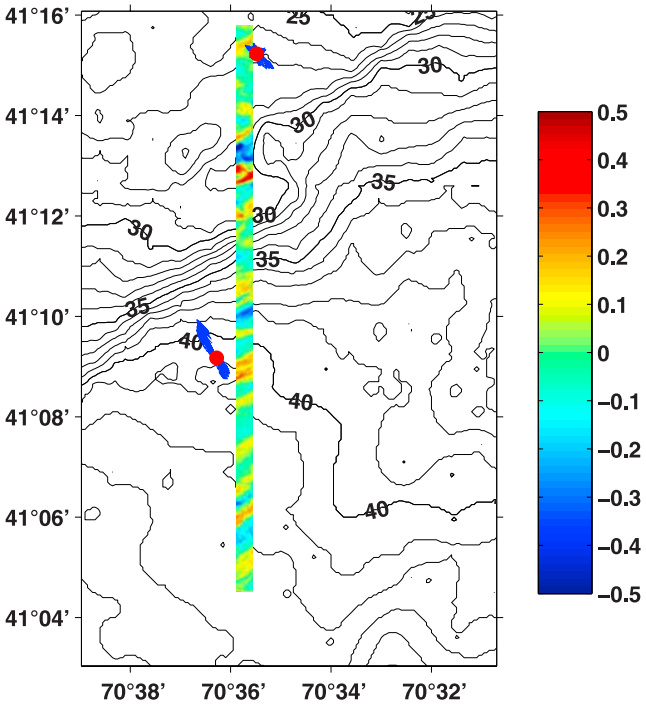

Figure 15. SST anomaly (°C) relative to 1.7-km along-track smoothed field. The solid red circles mark the positions of moored current meters, and the blue arrows are 20- to 60-min band-passed velocity vectors at depths of 9 m (northern mooring) and 8 m (southern mooring). The velocity vectors are expected to be normal to the internal-wave crests, and they can be seen to be approximately normal to the "crests" in the SST anomaly. (Adapted from *Edson et al.* [2007]; copyright American Meteorological Society.)

That is about 65–365 times smaller than the SST anomalies resulting from modulation of vertical mixing in the model experiment, but the modulation of the cool-skin effect could be larger if the internal wave can effectively modulate the thickness of the cool skin [*Osborne*, 1965].

[63] The simulated SST signal is largest during 15:00–20:00, and peak amplitudes are roughly ±0.08°C, which is smaller than some of the observed variability. The amplitude, frequency, and vertical profile of the imposed vertical velocity are expected to affect the size of the SST signal. Also, details of the warm-layer evolution and the size of the SST fluctuations are expected to depend sensitively on the parametrization of penetrating solar radiation. In the coastal waters where the CBLAST-Low field program was carried out, solar radiation is likely to attenuate more rapidly than in the *Paulson and Simpson* [1977]/Jerlov Type I parametrization used here (following *Price et al.* [1986]), so the warm-layer effect in the model may be underestimated. In any case, the model experiment demonstrates the feasibility of the *Walsh et al.* [1998] mechanism as a means of imprinting internal-wave signals on SST.

6. Conclusion

[64] A case study of SST variability in low-wind conditions, including times with and without a diurnal warm layer, was presented. Quasiperiodic SST variability was observed when the diurnal warm layer was present, and this SST variability was coherent with subsurface temperature fluctuations attributed to oceanic internal waves. A quasiperiodic SST pattern observed in airborne infrared imagery of the sea surface was observed to be oriented roughly perpendicularly to internal-wave velocity vectors, as expected if the SST patterns are a surface expression of the internal waves. The fact that the SST signal closely resembles the temperature signal observed in the bulk fluid indicates that the observed SST signal is not a result of any process involving the cool skin. Although the data presented here cannot directly confirm the hypothesis of *Walsh et al.* [1998] that an SST signal exists because internal waves modulate upper ocean mixing by modulating the depth of the diurnal warm layer, the data are consistent with this hypothesis, and a one-dimensional model experiment suggests that the hypothesized mechanism is plausible.

[65] Our failure to detect an internal-wave signal in the bulk-skin temperature difference obviously does not imply that the cool-skin straining mechanism cannot produce an observable SST signal. However, it does suggest that cool-skin straining by internal waves is a less effective mechanism than modulation of warm-layer physics for producing a signal in SST. Horizontal variability at internal-wave scales was observed in the skin temperature during the morning ship survey (Figure 6), and most of this variability is not reflected in the bulk temperature (not shown), suggesting that some of the internal-wave-scale variability is due to spatial variations in the cool-skin effect. These fluctuations in the skin temperature are incoherent with internal-wave temperature fluctuations in the main thermocline, but it is important to note that the horizontal temperature variability at the thermocline depends on the isotherm displacement (or time-integrated vertical velocity). Thus the ship survey data described here do not yield direct information about the vertical strain rate, making direct confirmation of the cool-skin straining hypothesis difficult. It would increase confidence that the variability in bulk-skin temperature difference observed during the morning ship survey was caused by internal waves if aerial infrared imagery showed coherent banded features in skin temperature during the morning survey. Unfortunately, aerial infrared imagery was not collected during the morning ship survey.

[66] *Zappa and Jessup*'s [2005] observations showed an internal-wave signal in SST at a time when there was no diurnal warm layer, so the warm-layer hypothesis of *Walsh et al.* [1998] cannot explain that signal. Some internal-wave signal is expected in the bulk-skin temperature difference [*Osborne*, 1965] (section 2), but the magnitude of this effect depends on the response of the cool-skin thickness to internal-wave straining, which is poorly understood. The skin-temperature signal observed by *Zappa and Jessup* [2005] was considerably smaller than the signals seen here and was associated with more energetic nonlinear waves. It is possible that the surface signal was due to modulation of the cool-skin effect, but it is also possible that those waves led to a signal in the bulk temperature that was merely reflected in the skin temperature. In this context, it is perhaps noteworthy that the model run (Figure 16) shows a very small, but measurable, surface temperature signal from a relatively weak internal wave during the night when no warm layer is

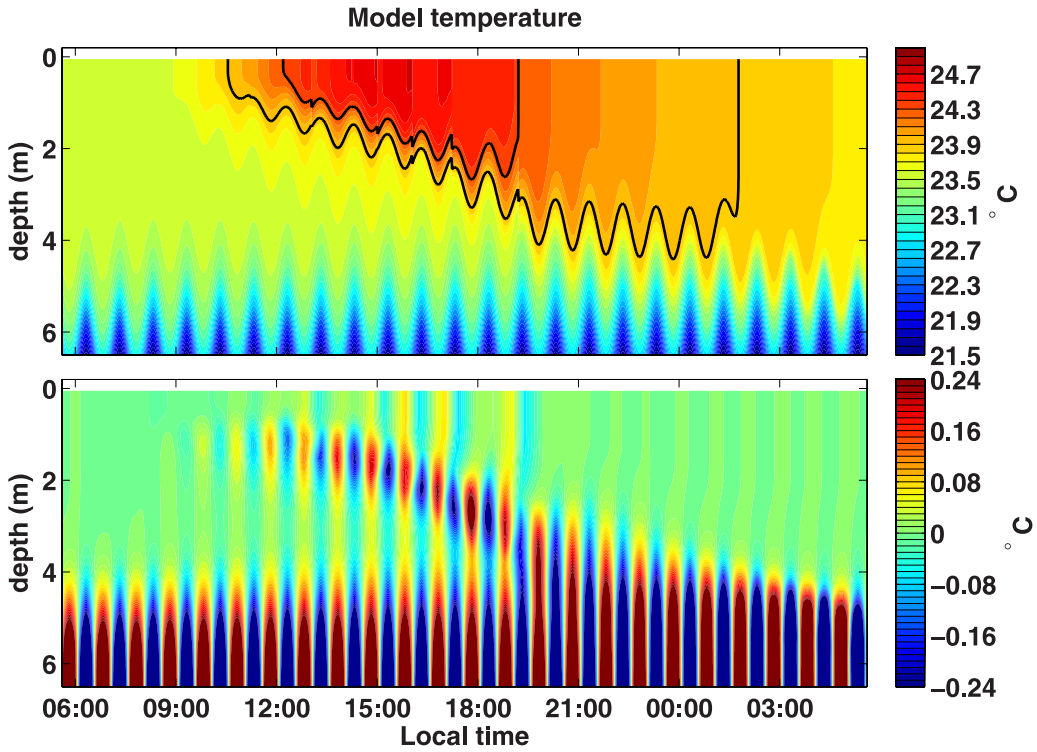

Figure 16. Results from a "thought experiment" using the *Price et al.* [1986] upper ocean model with an imposed internal-wave vertical velocity signal and the observed heat, momentum, and fresh water fluxes from one of the buoys. (top) Simulated temperature for 15–16 August 2003. The 23.9°C and 24.3°C isotherms are shown in black to illustrate isotherm discontinuities that result from vertical mixing in the model (e.g., between 15:00 and 18:00). (bottom) Simulated temperature, filtered to pass variations in the frequency band of the imposed vertical velocity signal. The fact that an appreciable signal in SST is produced by modulation of the depth of the warm-layer base suggests that the *Walsh et al.* [1998] mechanism is a plausible explanation of the observed signal.

present. In the model, modulation of vertical mixing is the only way that the internal wave can affect SST.

[67] Of course, there could be internal-wave effects other than vertical advection that might modulate the temperature of the warm layer. For example, the vertical shear of the horizontal velocity of the waves and its orientation to the wind-driven shear may serve to modulate near-surface mixing, or the wind-driven velocity may even "shear the tops off of the internal waves" to cause static instabilities. Nonlinear internal waves might also transport warm water at the wave phase speed to create a surface temperature signal, though such nonlinear transport would likely be accompanied by mixing [*Helfrich and Melville*, 2006].

[68] The fact that the early morning survey revealed no systematic relation between surface and subsurface temperature fluctuations suggests that the large signals observed from the ship and aircraft in the afternoon depend in some way on the presence of the warm layer. We are presently working with existing data to better understand the mechanism(s) by which internal waves produce a signal in SST, and we hope that future theoretical, observational, laboratory, and numerical studies will allow progress toward better understanding of the relationship between infrared observations of the sea surface and the dynamics beneath the surface. A coordinated field effort involving coincident infrared SST measurements, subsurface temperature and velocity measurements, and near-surface microstructure measurements (such as from the SkinDeEP instrument) [*Ward*, 2006] would allow considerable progress toward this goal.

Appendix A: Depth Estimation for Towed Instruments

[69] Mounting locations on the wire used to tow instruments from the FV *Nobska* were separated by 0.5 m, but the actual depths of the instruments varied in time as a result of slow variations in the angle of the wire (e.g., resulting from variations in the vessel's speed). Three of the subsurface instruments towed from the FV *Nobska* measured pressure. The 10th and 12th instruments were SBE 39 temperature/pressure recorders and a RBR DR-1050 was at the bottom of the "chain". Prior to analysis, all records were linearly interpolated to a common 4-s time base and the pressure records were used to estimate the actual depth of each instrument through time as follows.

[70] Given the nominal depth that each sensor would assume if the chain hung vertically, the angle from the surface to each of these 3 pressure measurements was estimated as $\cos^{-1}$(measured depth/nominal depth). This gives 3 estimates of the angle. Typically, the three estimates agreed to within 20°, and the largest angles were found for the deepest sensor. These three estimates were averaged to

obtain a single estimate for the angle of the chain with respect to the surface. (Although the chain is expected to take on something like catenary shape, the chain appeared to be straight in the upper few meters.) Finally, an offset (typically 0–0.5 m) was applied to ensure that the depth of sensor 10 (the shallowest pressure measurement) matched the value inferred from the observed pressure. The depth estimation method was "successful" in the sense that the estimated depth of the shallowest sensor agreed with visual estimates of the depth made from the deck of the FV *Nobska* during the surveys. The estimated depths are expected to be most accurate near the surface, where the angle of the line amounts to a small depth correction. This method of estimating the depth (mandated by the small number of pressure sensors) is obviously imperfect. However, inaccuracies in the estimated measurement depths do not affect the conclusions of this paper.

[71] **Acknowledgments.** We gratefully acknowledge funding for this research from the Office of Naval Research through the CBLAST Departmental Research Initiative (grants N00014-01-1-0029, N00014-05-10090, N00014-01-1-0081, N00014-04-1-0110, N00014-05-1-0036, N00014-01-1-0080) and the Secretary of the Navy/Chief of Naval Operations Chair (grant N00014-99-1-0090). We appreciate the leadership and dialogue provided by Jim Edson during CBLAST-LOW fieldwork and analysis. The excellent seamanship of Captain Matt Stommel and the crew of the FV *Nobska* proved vital to the success of shipboard operations during CBLAST-Low. The moored measurements and shipboard sampling relied heavily on the effort and expertise of Geoff Allsup, Paul Bouchard, Ryan Brown, Nan Galbraith, Brian Hogue, Dave Hosom, Lara Hutto, Jeff Lord, and Jason Smith of the WHOI Upper Ocean Processes group. We thank John Ambroult of Ambroult Aviation, Chatham, Massachusetts, for his flying services. Luc Rainville, Carlos Moffat, and two anonymous reviewers provided helpful comments on the manuscript. This is contribution 6998 from Lamont-Doherty Earth Observatory of Columbia University.

References

Anderson, S. P., R. A. Weller, and R. B. Lukas (1996), Surface buoyancy forcing of the mixed layer of the Western Pacific Warm Pool: Observations and 1D model results, *J. Clim.*, *9*, 3056–3085.

Apel, J. R. (1980), Satellite sensing of ocean surface dynamics, *Annu. Rev. Earth Planet. Sci.*, *8*, 303–342.

Castro, S. L., G. A. Wick, and W. J. Emery (2003), Further refinements to models for the bulk-skin sea surface temperature difference, *J. Geophys. Res.*, *108*(C12), 3377, doi:10.1029/2002JC001641.

Edson, J. B., et al. (2007), The Coupled Boundary Layers and Air-Sea Transfer Experiment in Low Winds (CBLAST-LOW), *Bull. Am. Meteorol. Soc.*, *88*(3), 341–356.

Fairall, C. W., E. F. Bradley, D. P. Rogers, J. B. Edson, and G. S. Young (1996a), Bulk parameterization of air-sea fluxes during TOGA COARE, *J. Geophys. Res.*, *101*, 3747–3764.

Fairall, C. W., J. S. Bradley, E. F. Godfrey, G. A. Wick, J. B. Edson, and G. S. Young (1996b), The cool-skin and warm-layer effects on sea surface temperature, *J. Geophys. Res.*, *101*, 1295–1308.

Fairall, C. W., E. F. Bradley, J. E. Hare, A. A. Grachev, and J. B. Edson (2003), Bulk parameterization of air-sea fluxes: Updates and verification for the COARE algorithm, *J. Clim.*, *16*, 571–591.

Farrar, J. T., and R. A. Weller (2006), Intraseasonal variability near 10°N in the eastern tropical Pacific Ocean, *J. Geophys. Res.*, *111*, C05015, doi:10.1029/2005JC002989.

Gasparovic, R. F., J. R. Apel, and E. S. Kasischke (1988), An overview of the SAR Internal Wave Signature Experiment, *J. Geophys. Res.*, *93*, 12,304–12,316.

Hagan, D. E., D. P. Rodgers, C. A. Friehe, R. A. Weller, and E. J. Walsh (1997), Aircraft observations of sea surface temperature variability in the tropical Pacific, *J. Geophys. Res.*, *102*, 15,733–15,747.

Helfrich, K. R., and W. K. Melville (2006), Long nonlinear internal waves, *Annu. Rev. Fluid Mech.*, *38*, 395–425.

Hill, K. L., S. Robinson, and P. Cipollini (2000), Propagation characteristics of extratropical planetary waves observed in the ASTR global sea surface temperature record, *J. Geophys. Res.*, *105*, 21,927–21,945.

Jessup, A. T., and V. Hesany (1996), Modulation of ocean skin temperature by swell waves, *J. Geophys. Res.*, *101*, 6501–6511.

Jessup, A. T., C. J. Zappa, M. R. Loewen, and V. Hesany (1997a), Infrared remote sensing of breaking waves, *Nature*, *385*, 52–55.

Jessup, A. T., C. J. Zappa, and H. Yeh (1997b), Defining and quantifying microscale wave breaking with infrared imagery, *J. Geophys. Res.*, *102*, 23,145–23,153.

Katsaros, K. B. (1980), The aqueous thermal boundary layer, *Boundary Layer Meteorol.*, *18*, 107–127.

Leighton, R. I., G. B. Smith, and R. A. Handlerb (2003), Direct numerical simulations of free convection beneath an air-water interface at low Rayleigh numbers, *Phys. Fluids*, *15*, 3181–3193.

Liu, A. K. (1988), Analysis of nonlinear internal waves in the New York Bight, *J. Geophys. Res.*, *93*, 12,317–12,329.

Marmorino, G. O., and G. B. Smith (2005), Bright and dark whitecaps observed in the infrared, *Geophys. Res. Lett.*, *32*, L11604, doi:10.1029/2005GL023176.

Marmorino, G. O., G. B. Smith, and G. J. Lindemann (2004), Infrared imagery of ocean internal waves, *Geophys. Res. Lett.*, *31*, L11309, doi:10.1029/2004GL020152.

Osborne, M. F. M. (1965), The effect of convergent and divergent flow patterns on infrared and optical radiation from the sea, *Dtsch. Hydrogr. Z.*, *18*, 1–25.

Paulson, C. A., and J. J. Simpson (1977), Irradiance measurements in the upper ocean, *J. Phys. Oceanogr.*, *7*, 952–956.

Price, J. F., R. A. Weller, and R. Pinkel (1986), Diurnal cycling: Observations and models of the upper ocean response to diurnal heating, cooling, and wind mixing, *J. Geophys. Res.*, *91*, 8411–8427.

Pritchard, M., and R. A. Weller (2005), Observations of internal bores and waves of elevation on the New England inner continental shelf during summer 2001, *J. Geophys. Res.*, *110*, C03020, doi:10.1029/2004JC002377.

Saunders, P. M. (1967), The temperature at the ocean-air interface, *J. Atmos. Sci.*, *24*, 269–273.

Schiller, A., and J. S. Godfrey (2005), A diagnostic model of the diurnal cycle of sea surface temperature for use in coupled ocean-atmosphere models, *J. Geophys. Res.*, *110*, C11014, doi:10.1029/2005JC002975.

Simpson, J. J., and C. A. Paulson (1980), Small-scale sea surface temperature structure, *J. Phys. Oceanogr.*, *10*, 399–410.

Stommel, H., and A. H. Woodcock (1951), Diurnal heating of the surface of the Gulf of Mexico in the spring of 1942, *Eos Trans. AGU*, *34*(4), 565–571.

Stommel, H., K. Saunders, W. Simmons, and J. Cooper (1969), Observations of the diurnal thermocline, *Deep Sea Res.*, *16*, 269–284.

Stumpf, H. G., and R. V. Legeckis (1977), Satellite observations of mesoscale eddy dynamics in the eastern tropical Pacific Ocean, *J. Phys. Oceanogr.*, *7*, 648–658.

Walsh, E. J., R. Pinkel, D. E. Hagan, R. A. Weller, C. W. Fairall, D. P. Rodgers, S. P. Burns, and M. Baumgartner (1998), Coupling of internal waves on the main thermocline to the diurnal surface layer and sea surface temperature during the Tropical Ocean-Global Atmosphere Coupled Ocean-Atmosphere Response Experiment, *J. Geophys. Res.*, *103*, 12,613–12,628.

Ward, B. (2006), Near-surface ocean temperature, *J. Geophys. Res.*, *111*, C02004, doi:10.1029/2004JC002689.

Wick, G. A., J. C. Ohlmann, C. W. Fairall, and A. T. Jessup (2005), Improved oceanic cool-skin corrections using a refined solar penetration model, *J. Phys. Oceanogr.*, *35*, 1986–1996.

Zappa, C., and A. T. Jessup (2005), High-resolution airborne infrared measurements of ocean skin temperature, *IEEE Geosci. Remote Sens. Lett.*, *2*(2), 146–150.

Zappa, C. J., W. E. Asher, and A. T. Jessup (2001), Microscale wave breaking and air-water gas transfer, *J. Geophys. Res.*, *106*, 9385–9391.

Zappa, C. J., W. E. Asher, A. T. Jessup, J. Klinke, and S. R. Long (2004), Microbreaking and the enhancement of air-water transfer velocity, *J. Geophys. Res.*, *109*, C08S16, doi:10.1029/2003JC001897.

J. T. Farrar and R. A. Weller, Department of Physical Oceanography, Woods Hole Oceanographic Institution, Mail Stop 29, Woods Hole, MA 02543, USA. (jfarrar@whoi.edu)

A. T. Jessup, Applied Physics Laboratory, University of Washington, Seattle, WA 98195, USA.

C. J. Zappa, Lamont-Doherty Earth Observatory, Columbia University, Palisades, NY 10964, USA.